Indian J. Phys. **73B** (3), 423-461 (1999)

IJP B
an international journal

Radio environment over Indian east coast : a combined study from sodar observations and radiosonde measurements

Swati Choudhury

Machine Intelligence Unit, Indian Statistical Institute,
203 B. T Road, Calcutta-700 035, India

and

D Dutta Majumder[1]

Electronics and Communication Science Unit, Indian Statistical Institute,
203 B. T Road, Calcutta-700 035, India

Received 31 December 1998, accepted 23 March 1999

Abstract · An *a priori* knowledge of radio-climatology of the lower atmosphere over a region plays an extremely significant role in maintaining the reliability and performance of various radio-communication systems operating in the high frequency ranges (VHF/UHF/SHF/EHF). Keeping this in mind, we have planned to investigate the radio-climatological properties over Calcutta using radiosonde (an *in-situ* technique) and a 2350 Hz monostatic sodar system (an acoustic remote sensing technique). Radiosonde data are analyzed to estimate the percentage occurrence of radiorefractivity, radiorefractivity gradients (sub-refraction, normal-refraction, super-refraction and ducting) which are the key parameters to visualize and understand the phenomena of radiowave propagation. Sodar data are also analyzed to estimate the percentage occurrence of different kind of layer structures appeared in the Lower Planetary Boundary Layer (LPBL) during different months and seasons over our site of observation. Finally, the conclusion and application emerged out from the obtained results are discussed.

Keywords : Radio-climatology, *in-situ* technique, remote sensing technique

PACS Nos. : 92.60.Fm, 92.60.Ry

1. Introduction

The reliability and performance of various communication systems (such as Radars, Microwave Communication systems, *etc.*) operating in VHF/UHF/SHF/EHF ranges are critically dependent on the radio-climatic properties of the lower atmosphere. Atmospheric properties involve both

[1] e-mail : ddm@isical.ac.in

temporal and spatial changes due to continuous variation in temperature (T), pressure (p), humidity (e) and radio-refractivity (N). Variations in these atmospheric parameters may affect the reliability of various communication systems in different ways. Therefore, to set up a reliable communication link (LOS link, Troposcatter system *etc.*) an *a priori* knowledge of the properties of the corresponding radio environment (under which the system is operating) is essential.

To perform this task, now a days a variety of *in-situ* and remote sensing techniques are available which are being used successfully all over the world to extract the radioclimatic properties on a regular and discrete basis. To undertake radio-climatic studies over a region, sometimes the use of a single instrument cannot fulfill the objectives, under such situation use of multi sensor techniques are advisable. But simultaneous application of several techniques is an expensive matter. To make a compromise, we have chosen a combination of *Sodar System* (acoustic remote sensing technique) and *Radiosonde Technique* (*in-situ* technique) for our study. We have designed a 2350 Hz monostatic sodar system at the Electronics and Communication Science Unit of Indian Statistical Institute, Calcutta (India) and recorded the observation on regular basis to deduce the climatology over our site of experiment. We have collected the radiosonde data at regular basis for the year 1986-87 (at 0530 hrs IST and 1730 hrs IST) from nearby station (Dum Dum Air Port, Calcutta).

In India, most of the studies on radio-climatology and radiowave propagation have been carried out mainly over the northern and southern region which were mostly worked out by the scientists from the National Physical Laboratory, New Delhi (India). A survey on existing literature reveals that over the eastern coastal region of India these types of studies have not been carried out on a wide scale, notwithstanding the fact that this region experiences very prominent diurnal, monthly and seasonal changes. Keeping this in mind, a research group at Electronics and Communication Science Unit of Indian Statistical Institute (Calcutta) started working in this area since mid eighties [1-5].

In this paper, initially we will discuss the results obtained from the analysis of Sodar observations recorded during different months and seasons over the eastern coastal region of India. Radiorefractivity (N), and radio-refractivity gradient (ΔN) are the key parameters to understand properly the radio-climatology of a particular region which in turn explain the phenomena of radiowave propagation. Therefore in the next part of this paper, we will present a brief introduction on radio-refractivity, radio-refractivity gradients, radio-refractivity profile, different units and their gradients. In addition to this a discussion on previous work on radio-climatology will be presented.

We have analyzed the collected radiosonde data to gather information about the monthly and seasonal variations of surface refractivity N_s, refractivity gradients ΔN, percentage occurrences of sub-refraction, normal refraction super-refraction and ducting. The obtained results are discussed and finally the application and conclusion emerged out from this work are presented.

2. Sodar observations recorded at Calcutta

We have recorded the sodar observations for the year 1986 and 1987 using a 2350 Hz monostatic sodar system and estimated the percentage occurrence of various types of structures, observed at our site of experiment.

2.1 Occurrence probability of sodar structure :

The occurrence probabilities of various type of sodar structures are showed in Figure 1. It is observed that thermal echoes occurred for 33.8%, shear echoes for 61.3% and there is no structure for 4.9% of time. Further subdivision shows that thermal plumes occur for 29.1%, rising layer occur for 4.7%, surface based layer (with uniform top) for 6.7%, surface based layer (with short spike) for 23.4%, surface based layer (with tall spike) for 16.2%, stratified layer (non-undulating) for 7.2%, stratified layer (undulating) for 5.9% and stratified layer (with dot echoes) for 1.9% of time.

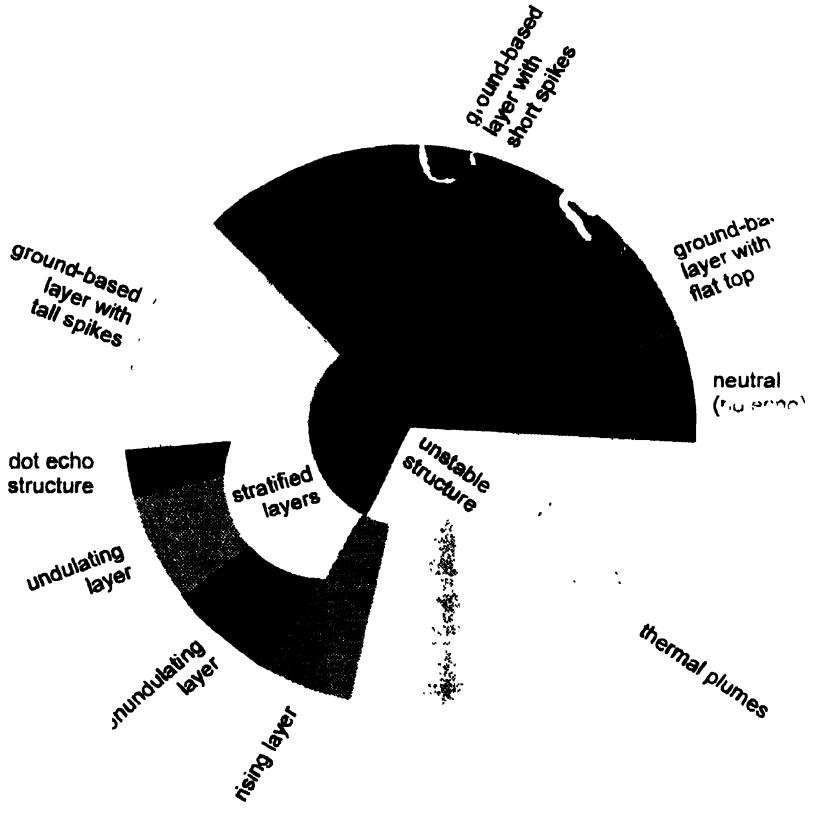

Figure 1. Percentage occurrence of different types of sodar structures, observed at Calcutta.

2.2 Sodar observations observed after sun-set :

After the disssipation of thermal plumes, the atmosphere becomes homogeneous for some time and no echo returns are observed on the chart paper. Gradually, the earth surface emits the absorbed heat in the form of infrared radiations. Emission of these infrared radiations initiates the formation of ground-based temperature inversion layer. Though there exist several causes of formation of inversion layer, the above described cause is one of the basic ones. For the sake of convenience, in further discussion we will use ground-based or surface layer in place of ground-based temperature inversion layer.

We have observed that the mean depth of the ground-based layer has experienced diurnal, monthly and seasonal variations. We have analyzed sodar data (recorded on continuous

basis) collected over two years to estimate the diurnal, monthly and seasonal variation of mean depth of the ground-based layer. Figure 2 shows the monthly distribution of the mean depth of ground-based layer.

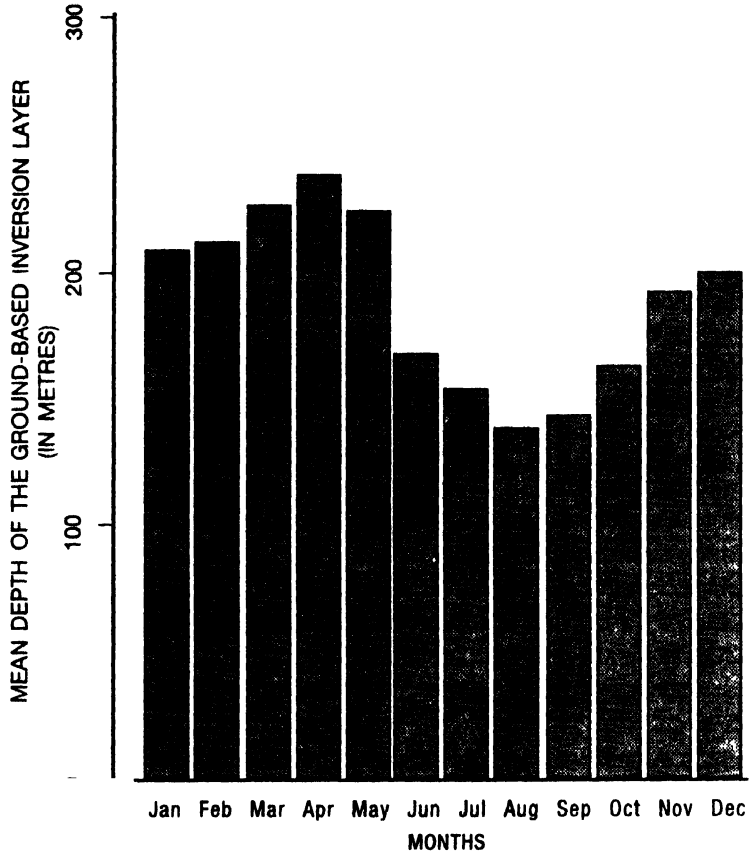

Figure 2 The monthly variation of the mean depth of the ground-based layer

It is clear from this figure that the mean depth has increased between January and May. The maximum value of mean depth has been observed during the month of April (237.0 meters). Further investigation reveals that the mean depth has decreased between the months of May and September. The month of August (139.0 meters) has experienced the minimum value of mean depth of the ground-based layer. Again a continuous increase in mean depth has been observed between the months of September and December. As far as the seasonal behavior is concerned, the mean depth of ground-based layer is maximum and minimum during the pre-monsoon and monsoon season respectively. On the other hand, value of the mean depth of ground-based layer during the winter season is greater than that of post-monsoon season.

Figure 3 describes the diurnal variation of the mean depth of ground-based layer. It can be seen that the mean depth of ground-based layer has increased between 1800 and 2400 hrs IST and has decreased gradually between 2400 and 0600 hrs IST. The mean depth is the maximum between 2300 and 2400 hrs IST whereas it is the minimum between 0500 and 0600 hrs IST.

So far we have discussed the diurnal, monthly and seasonal variation of the mean depth of ground-based layer. The continuous observation on sodar data reveals that on many occasions the ground-based layers are associated with flat top, small spikes, tall spikes, elevated layers and wave motion *etc*. In the earlier discussion, we have already presented the relative percentage occurrence of these structures estimated on yearly basis. In this section, we will discuss the monthly variation of percentage occurrence of these different types of structures to find out more detail information.

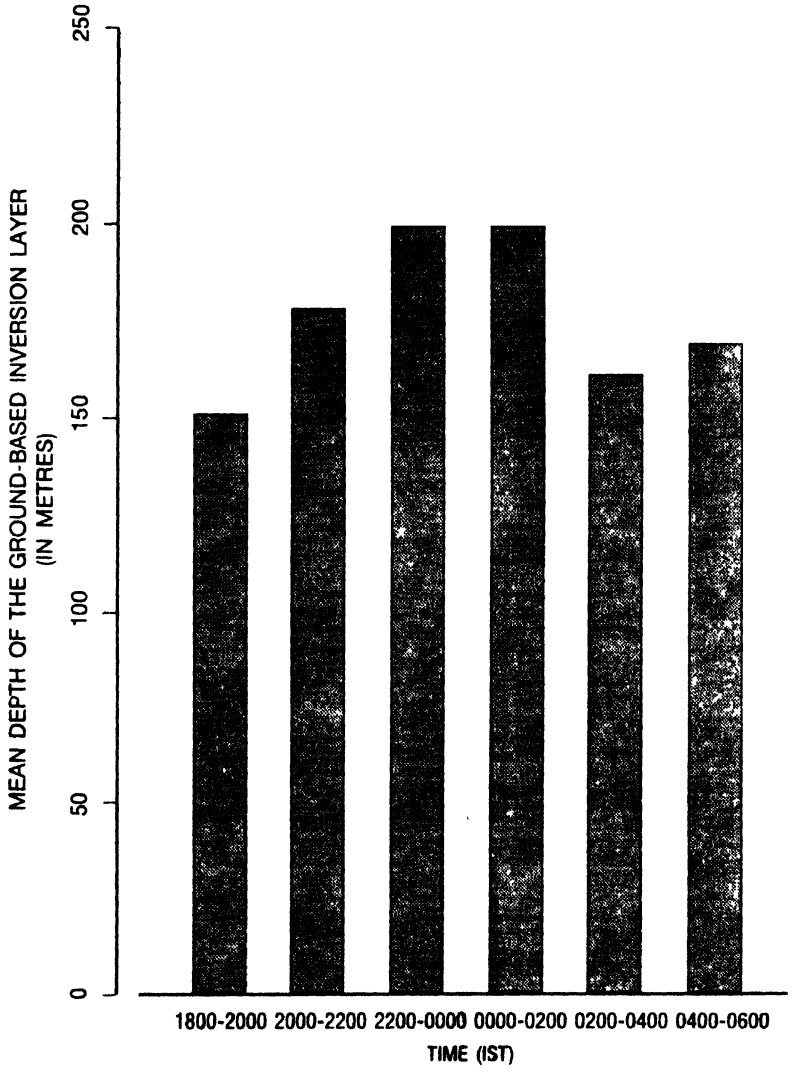

Figure 3. Diurnal variation of the mean depth of the ground-based layer

Figure 4 presents the monthly variation of percentage occurrence of ground-based layer with uniform or flat top. We can study from this figure that the percent occurrence of ground-based layer with flat top is maximum during the month of January whereas, it attains nil value during the months of May and August. On the other hand, during the months of June

and December, the corresponding percentage occurrences of ground-based layer with flat top are comparatively greater than that of the rest of the months.

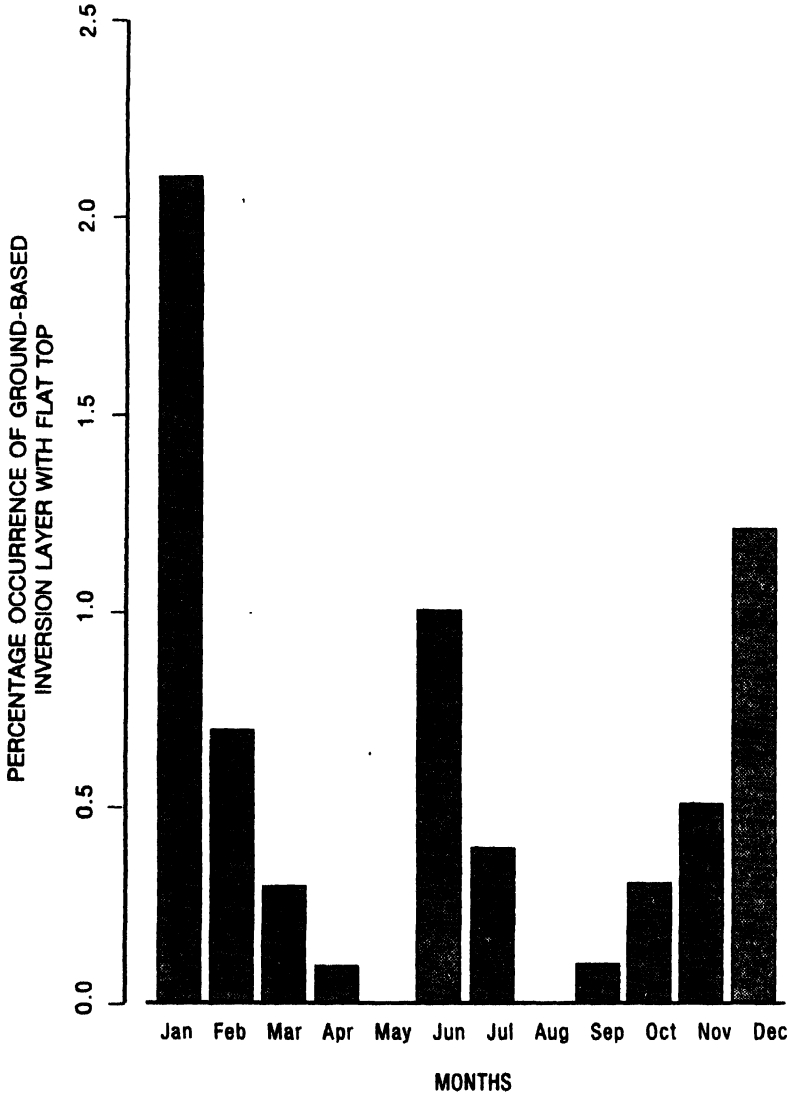

Figure 4. The monthly variation of the percentage occurrence of ground-based layer with flat top.

Figure 5 describes the monthly variation of percentage occurrence of ground-based layer with small spikes. It can be seen from this figure that during the pre-monsoon and the monsoon months the percentage occurrence of ground-based layer with small spikes are greater with respect to the rest of the months. A continuous fall in percentage occurrence has been observed between the months of August and December. Further study reveals that the percentage occurrence of ground-based layer with small spikes is the maximum during the month of May whereas it is the minimum during the month of December.

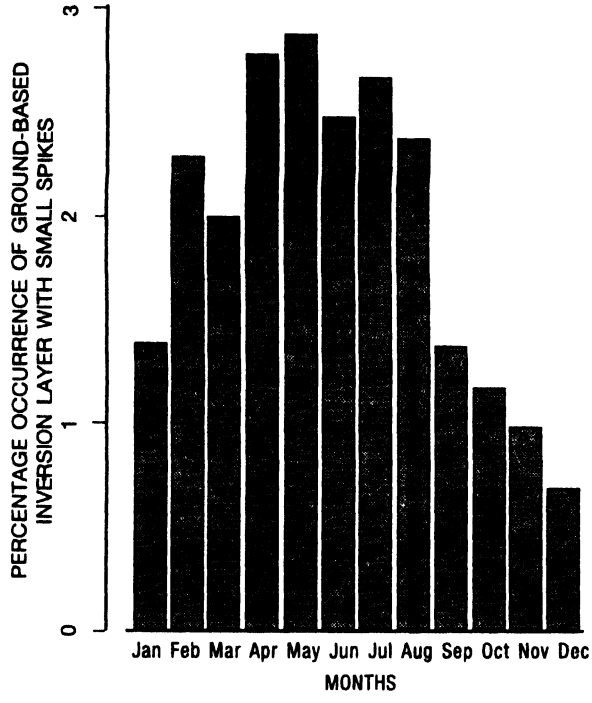

Figure 5. The monthly variation of percentage occurrence of the ground-based layer with small spikes

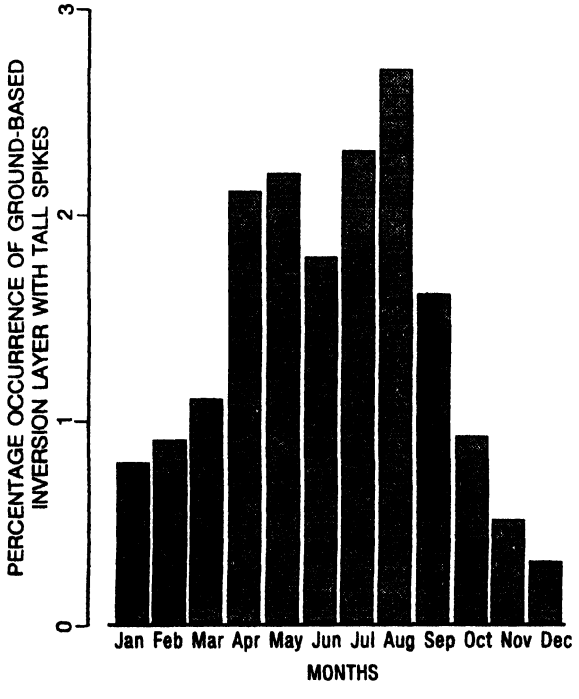

Figure 6. The monthly variation of the percentage occurrence of ground-based layer with tall spikes.

The monthly variation of percentage occurrence of the ground-based layer with tall spikes is shown in Figure 6. This figure describes that ground-based layer with tall spikes has been formed during all the months but there exist å significant differences in their percentage occurrence. A continuous increase in percentage occurrence followed with slight fall in the month of March has been observed between the months of January and May. Similarly a continuous decrease in percentage occurrence has been noticed between the months of July and December. Finally, it can be concluded that the ground-based layer with tall spikes has been formed for greater percent of time during the months of April, May and June, whereas it has occurred for a lesser percent of time during winter months.

Figure 7 represents the monthly variation of percentage occurrence of ground-based layer associated with dot echo structure. The probability of formation of dot echo structure is nearly nil during the winter and the pre-monsoon months whereas during the monsoon and the

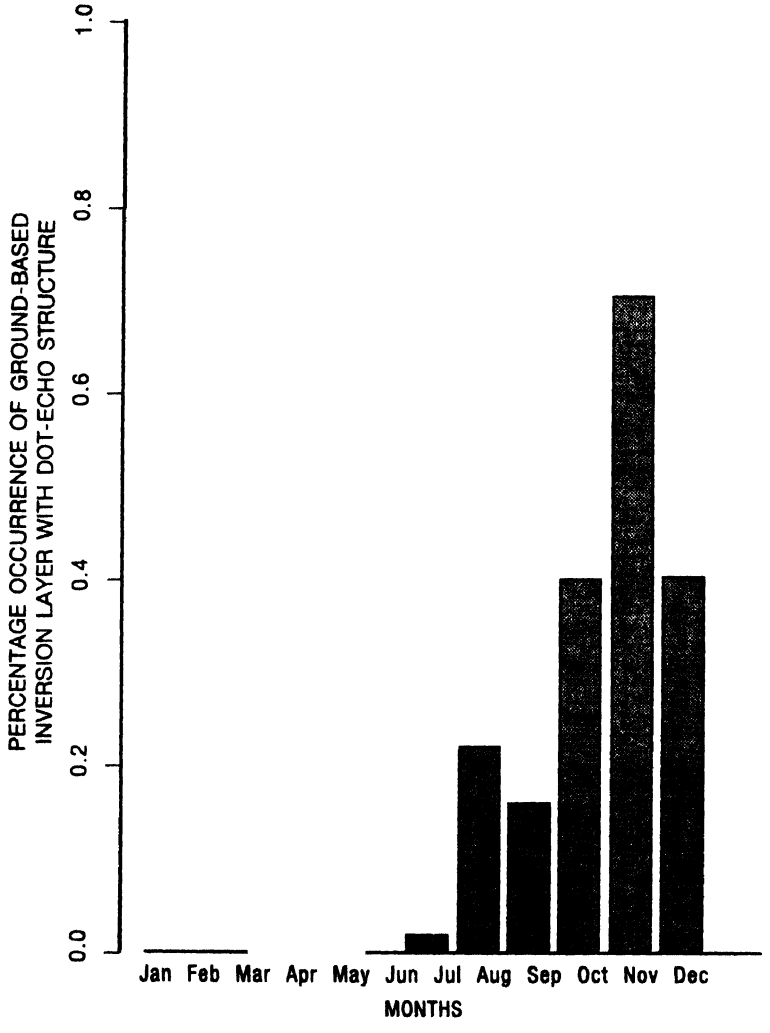

Figure 7. The monthly variation of percentage occurrence of ground-based layer associated with dot echo structure.

post-monsoon months it has occurred with greater percent of time. The probability of formation of dot echo structure is the highest during the month of July.

The monthly variation of the percentage occurrence of ground-based layer associated with elevated layer is shown in Figure 8. It can be studied from this figure that the probability of formation of elevated layer is negligible during the monsoon months whereas, it has occurred prominently during the pre-monsoon and the post-monsoon months.

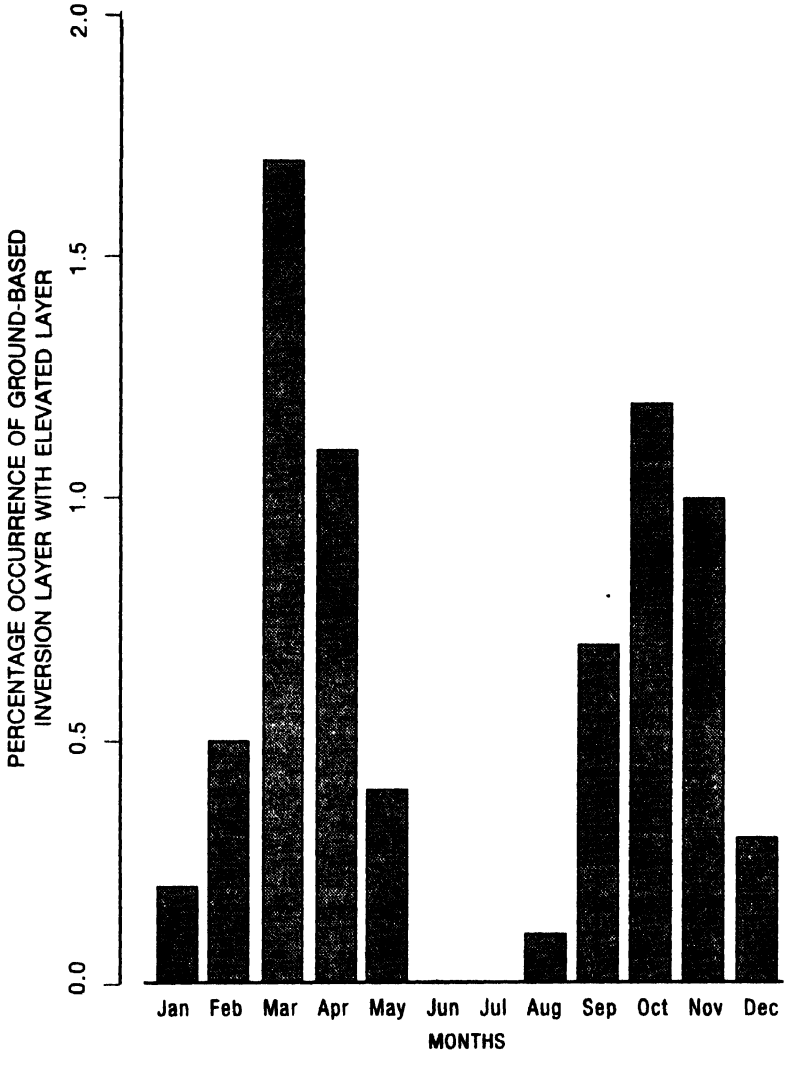

Figure 8. The monthly variation of the percentage occurrence of ground based layer associated with elevated layer.

The diurnal variation of percentage occurrence of the elevated layer is depicted in Figure 9. This result suggests that about 66.2% of the elevated layer has occurred between 2200 and 0400 hrs IST. The percentage occurrence of elevated layer has increased between 1600 and 0400 hrs IST and has decreased continuously between 0400 and 0600 hrs IST.

Figure 10 has been drawn to study the percentage occurrence of mean depth of the elevated layer. It can be studied from the figure that more than 65% of the elevated layers are occurred between 30 and 60 meter. About 10.8% of the elevated layers have occurred between 60 and 100 meter, whereas rest of the elevated layers are seen to exist between 0 and 30 meter. Further investigation reveals that the percentage occurrence of elevated layer is highest between 40 and 50 meter range.

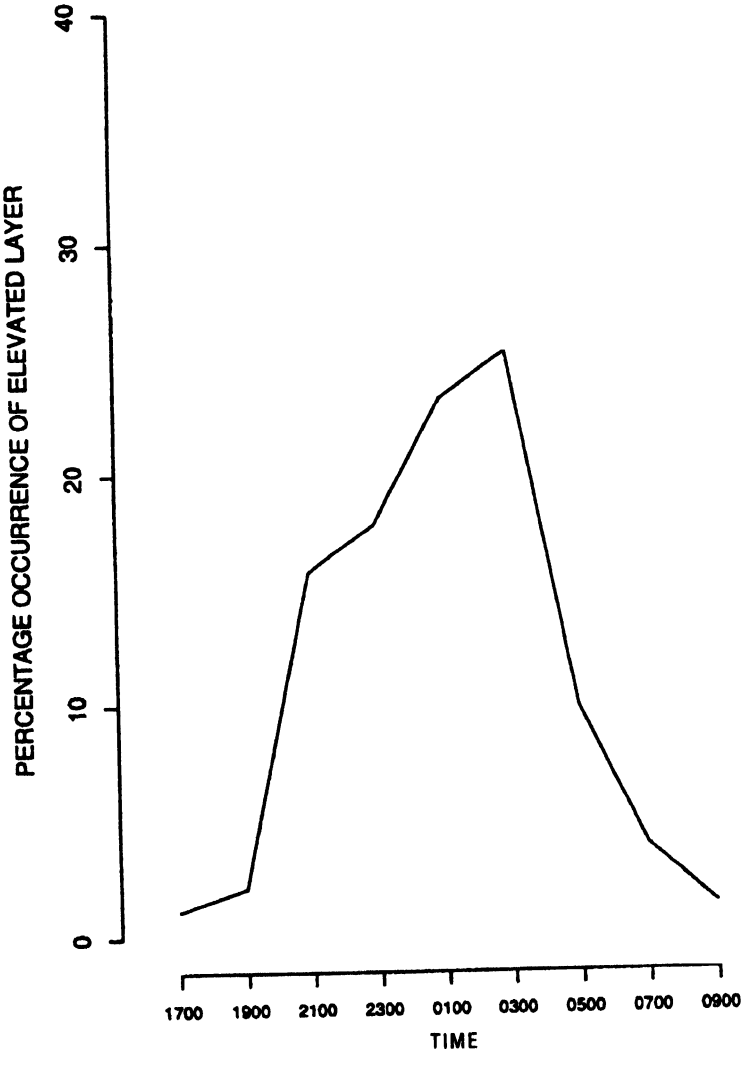

Figure 9. Diurnal variation of percentage occurrence of the elevated layer

We have discussed in Chapter 3 of Ref. [5] that on many occasions, ground-based and elevated layer have experienced wave motion. A continuous observation on sodar data reveals that percentage occurrence of these wave like structures have shown significant monthly variation.

Figure 11 describes the monthly variation of percentage occurrence of these wave-like structures appeared on sodar record. It is clear from this figure that these wave-like structures have occurred dominantly during the pre-monsoon and the post-monsoon months whereas, during monsoon months probability of formation of such structures are nearly nil.

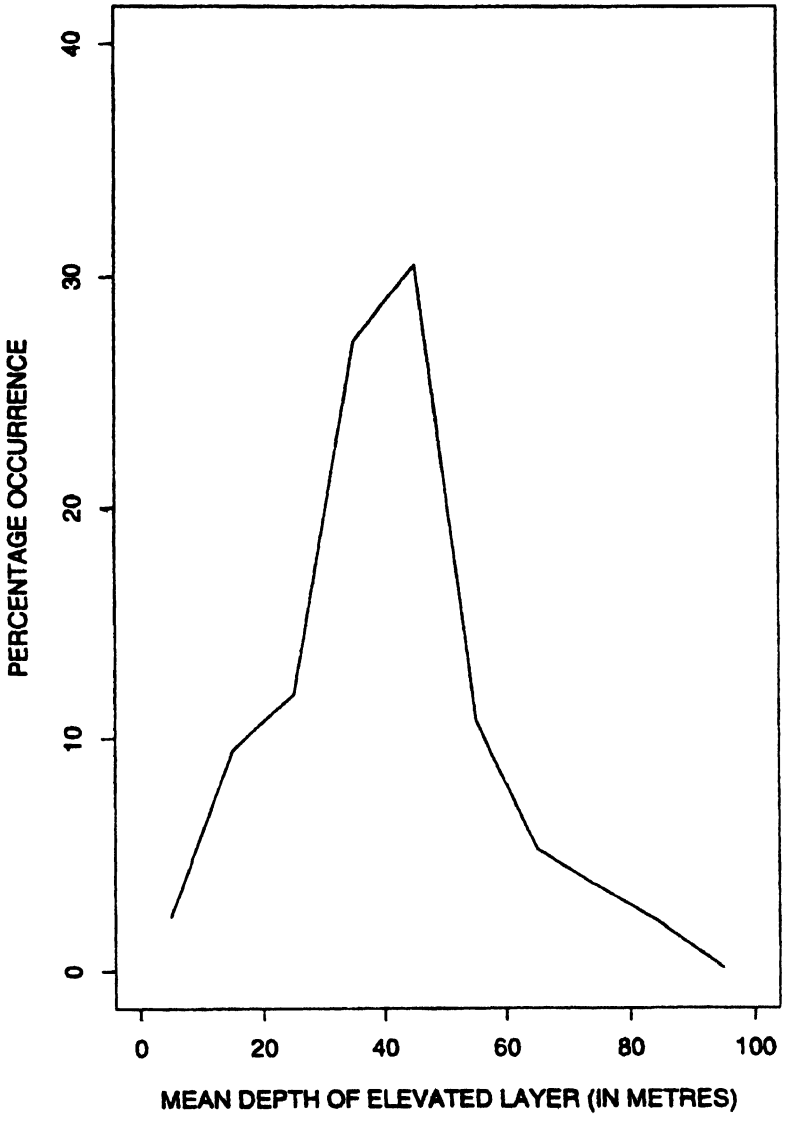

Figure 10. The percentage occurrence of the mean depth of elevated layer.

2.3 Sodar observations observed after sunrise :

During the morning hours, solar radiations erode the surface based inversion layer (which forms during night hours) and gradually this layer starts rising from the ground. With continuous solar heating, the ground based inversion layer rises sufficiently high and after sometime it becomes insensitive to sodar detection. This layer is called *rising inversion layer.*

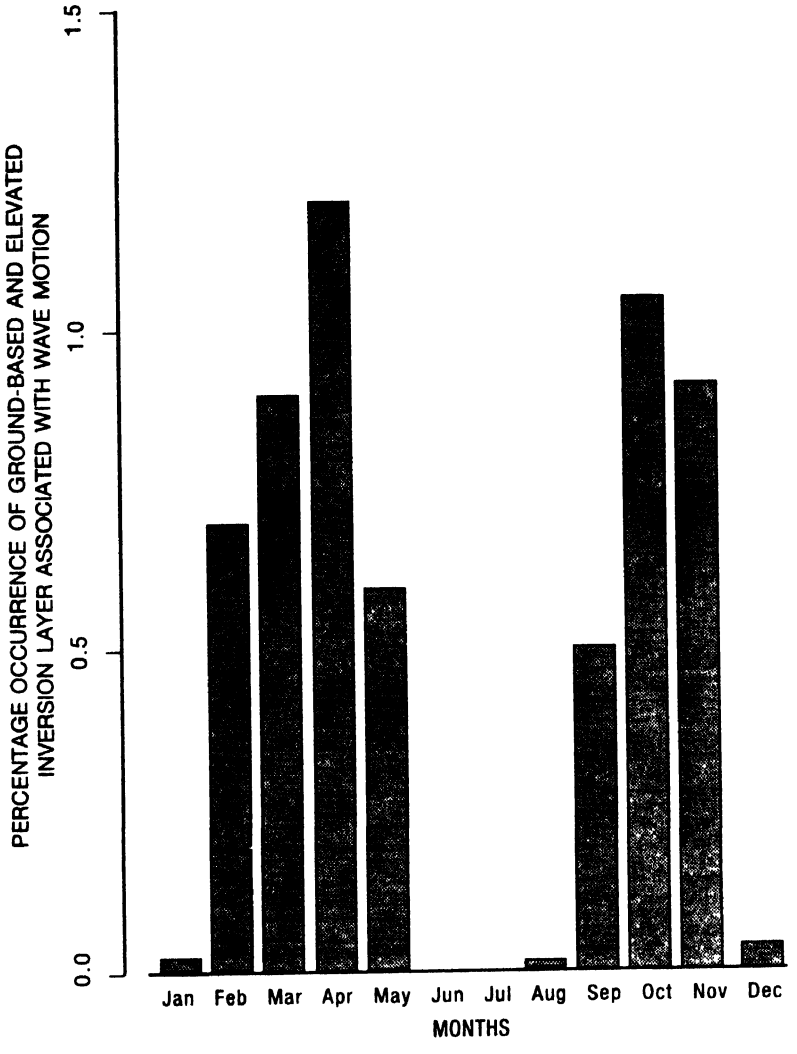

Figure 11 The monthly variation of the percentage occurrence of wave-like structure appeared on the sodar record.

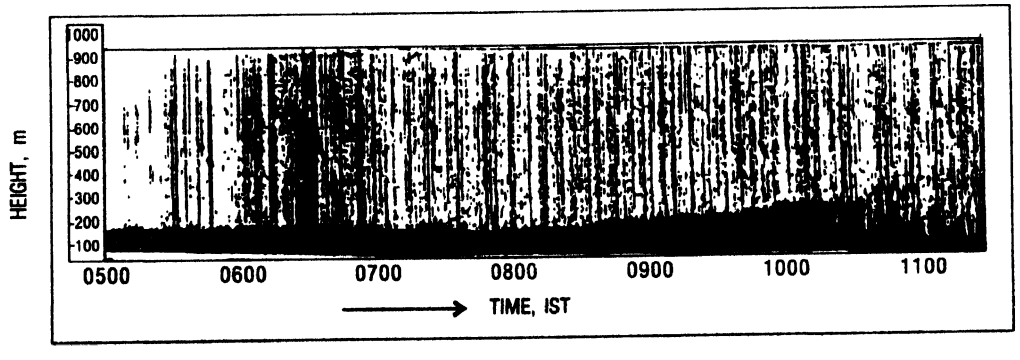

Figure 12. Sodar record of the rising inversion layer

Figure 12 shows the rising inversion layer observed at our site of experiment. After sunrise, average time required to erode the ground based inversion layer completely, differs from month to month and season to season. On the basis of two years data, we have estimated the average time required after sunrise to erode the ground based layer, during different months and seasons in Calcutta. Seasonal study reveals that after sunrise, to erode the surface based inversion layer, winter and monsoon season take the maximum and minimum time respectively. Average time required to erase the surface based layer completely during winter, pre-monsoon, monsoon and post-monsoon seasons are 250.8 minutes, 212.5 minutes, 175.5 minutes and 236.6 minutes, respectively.

Figure 13 shows the average time required after sunrise to erase the ground based layer during different months in Calcutta. Monthly study shows that average time required after

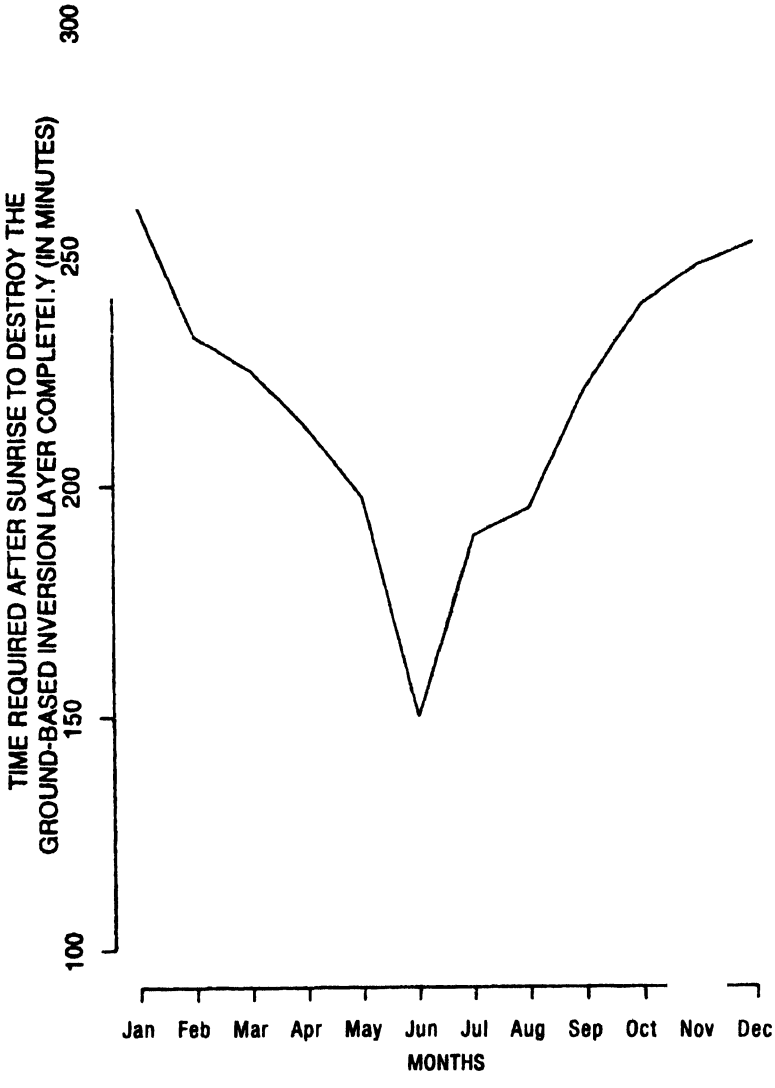

Figure 13. The average time required, after sunrise to erase the ground-based layer completely.

sunrise to erase the ground-based-layer is the maximum and the minimum during the month of January and June respectively. This result indicates that during the morning hour of winter season (time period of rise of surface based layer) probability of interference from distant transmitters (working mainly at microwave and higher frequency region) will be high as it takes the maximum time to erase the ground based layer whereas, probability of such kind of interference will be least during the monsoon season, as it takes the minimum time to erase the surface based layer after sunrise.

Apart from this, we can also speculate the behavior of various pollutants ejected from different factories, industries, house fire *etc.* From the above result we have observed that winter season takes the maximum time after sunrise to erode the ground based layer completely. Therefore, during this season various pollutants trapped under the ground based layer will take longer time to get dispersed from lower level to higher level. Similarly, during the morning hour of monsoon season, it will take the minimum time after sunrise to disperse the various pollutants from lower level to higher level. This result has got very useful application in order to control the environmental pollution upto a certain limit. On the basis of this result, working hours of different factories and industries can be fixed for different seasons over a particular region. Thus for instant, during the morning hour of winter season, various factories and industries must be allowed to start working late, so that the ground based inversion layer may get erased completely whereas, during monsoon season they may start working at least one and half hour earlier than that of winter season. Finally, it is expected that these kind of precautions will be effective to check the environmental pollution upto a certain extent.

We have estimated the coefficient of correlation between average plume height and plume duration during the different hour of convection. Figure 14 shows the plot of coefficient of correlation with respect to time between the time period 1100 and 1500 hrs IST. This figure describes that during initial hour (1100-1200 hrs IST) there exist a positive correlation between the average plume height and duration *i.e.* taller the average plume height, longer the plume duration. Between 1200 and 1300 hrs a continuous decrease in the coefficient of correlation has been noticed and between 1300 and 1400 hrs there exist a negative correlation between average plume height and duration *i.e.* taller the plume height and shorter the plume duration. Further investigation reveals that between 1400 and 1500 hrs, again there exist a positive correlation between average plume height and plume duration. Sodar observations show that during this time the average plume duration increases with a small decrease in average plume height. Consequently there exist a positive correlation between average plume height and plume duration *i.e.*, still higher the average plume height, longer the plume duration. This result indicates that during the initial hours of formation of thermal plume (between 1100 hrs and 1200 hrs) the depth of mixing is high but the speed of mixing process is low (because the most of the solar energy is used in breaking the ground based inversion layer). Between 1200 and 1400 hrs IST, the depth of mixing and speed of mixing process both are high. On the other hand, during later hours, speed of mixing process decreases with small decrease in average mixing depth. This result also has got very useful application in order to check the environmental pollution upto a certain extent. On the basis of above result, it can be concluded that time between 1200 and 1400 hrs IST must be considered as most suitable time for different chemical factories,

industries and refineries to throw off their waste, harmful gases and pollutants into the atmosphere. It is expected that due to high mixing depth and high mixing speed pollution density will be least during this time period.

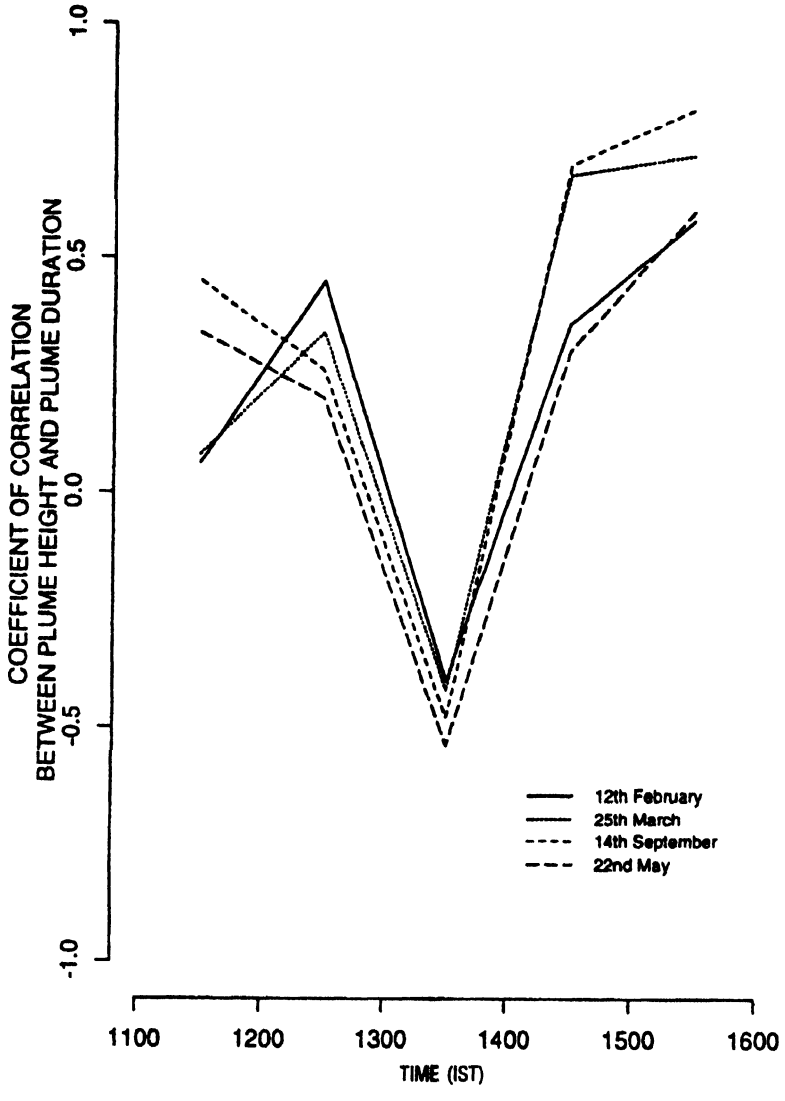

Figure 14. The variation of the coefficient of correlation (estimated between the average plume height and the plume duration) during the different time of convection.

3. Tropospheric radio refractivity

For a mixture of gases the extent by which the refractive index is greater than 1 can be expressed as follows :

$$n-1=\sum m_i\left(A_i+\frac{B_i}{T}\right), \tag{1}$$

where

m_i = density and

T = the absolute temperature.

A_i and B_i are two constants of which the second is only non-zero for gases whose molecules have an electric dipole moment, *e.g.*, water vapor.

Since $n - 1$ is very small, we use a quantity N which is 10^6 times greater and is called *refractivity* or *coindex of refraction.*

$$N = (n-1) \times 10^6 . \tag{2}$$

The refractivity N is a function of temperature, pressure and humidity. In troposphere, we need to consider only the effects of CO_2, dry air (non-polar gases) and water vapor (polar gas). Thus for practical application, one can write the equation for refractivity N, as follows [6, 7]:

$$N = \frac{K_1 P_d}{T} + \frac{K_2 e}{T} + \frac{K_3 e}{T^2} + \frac{K_4 P_c}{T}, \tag{3}$$

where K_1, K_2, K_3 and K_4 are constants,

P_d = pressure of dry air,

e = partial pressure of water vapor and

P_c = partial pressure of CO_2.

Substituting the values of constants, the eq. (3) becomes [8]

$$N = 77.6 \frac{P}{T} + 3.75 \times 10^6 \frac{e}{T^2} \tag{4}$$

$$= \frac{77.6}{T}\left(P + \frac{4810\, e}{T}\right), \tag{5}$$

where

P = atmospheric pressure in mb,

e = water vapor pressure in mb and

T = absolute temperature in degree kelvin.

In the right hand side of eq. (4) and (5), the first term is called *dry term* and the other as *wet term* [9].

This expression of radio-refractivity is valid upto 100 GHz with an error, less than 0.5%.

In radio-meteorology, sometimes it becomes useful to employ the concept of potential value of refractive index referred to some standard pressure level. By replacing the values of pressure, temperature and vapor pressure in the expression for N with their values at some desired pressure level, the potential refractive index or the potential refractive modulus can be defined as [10]

$$\phi = \frac{77.6}{\theta}\left[P_0 + 4810\frac{C_0}{\theta}\right], \tag{6}$$

where

θ = is the potential temperature,

C_0 = the potential partial pressure of water vapor, both referred to reference pressure P_0.

The potential temperature is defined as

$$\theta = T\left(\frac{P_0}{P}\right)^{\frac{R}{mC_p}}, \tag{7}$$

where

R = universal gas constant,

m = the molecular weight of air and

C_p = specific heat of air at constant pressure

and

$$C_{\wedge} = C\left|\frac{P_0}{P}\right|.$$

4. Radiorefractivity profiles : Different units and their gradients

Long term studies and experiments in the area of radio-meteorology have given a scope to represent the refractivity profiles in terms of various units. The most commonly used ones are :

(i) *B Unit*

(ii) *M Unit*

(iii) *A Unit and*

(iv) N_0 *Unit.*

(i) B (h) Unit :

To define the $B(h)$ unit of radio-refractivity, one has to first consider the concept of *effective earth radius factor.* This concept makes 'straight' the actual curved path of a radio ray in the atmosphere by presenting it relative to an imaginary earth larger in radius by a factor k than the radius of the real earth. By maintaining the relative curvature between earth and the radio ray, mathematically it can be expressed as :

$$\frac{1}{a} + \frac{1}{n}\frac{dn}{dh}\cos\theta = \frac{1}{ka} + 0. \tag{8}$$

Curvature of earth + Curvature of Radio ray =

Curvature of effective earth + Curvature of straight ray.

Solving eq. (8), we get

$$k = \frac{1}{1 + \frac{a}{n}\frac{dn}{dh}\cos\theta}. \tag{9}$$

For rays tangential to earth *i.e.*, $\theta = 0$ and assuming n equal to unity, the expression for k eq. (9) can be approximated as :

$$k \simeq - \frac{1}{1 + a\frac{dn}{dh}}. \tag{10}$$

By setting $\frac{dn}{dh} = -\frac{1}{4a}$ in eq. (10) we get $k = \frac{4}{3}$. This value of $k = \frac{4}{3}$ defines the *standard atmospheric condition.* Finally to define $B(h)$ unit, one may remove the standard decrease of N with height by adding a quantity SN to $N(h)$ where

$$SN = \frac{h}{4a} \times 10^6.$$

Thus obtaining the $B(h)$ unit as

$$B(h) = N(h) + SN, \tag{11}$$

$$B(h) = \left[(n-1) + \frac{h}{4a}\right] 10^6 = N(h) + \frac{h}{4a} \times 10^6 \tag{12}$$

and the gradient of B can be expressed as

$$\frac{dB(h)}{dh} = \frac{dN(h)}{dh} + \frac{1}{4a} \times 10^6.$$

(ii) M(h) Unit :

By setting $\frac{dn}{dh} = -\frac{1}{a}$ in eq. (10) we get $k = \infty$ or an *effective earth of infinite radius.* This implies that the earth is flat and the communication is taking place between the radio visible terminals. Thus by adding a quantity

$$\delta N = \frac{h}{a} \times 10^6$$

to $N(h)$, one can define the modified index of refractivity as

$$M(h) = N(h) + \delta N = \left[n - 1 + \frac{h}{a}\right] \times 10^6 = N(h) + \frac{h}{a} \times 10^6. \tag{13}$$

$M(h)$ is also termed as *refractive modulus* or *modified refractivity.* Gradient of M can expressed as

$$\frac{dM(h)}{dh} = \frac{dN(h)}{dh} + \frac{1}{a} \times 10^6 . \tag{14}$$

This approach is very useful in studying phenomena of *extended ranges of radio waves.*

(iii)A(h) Unit :

This has been observed that, both $B(h)$ and $M(h)$ units are defined on the basis of effective earth radius model. Derivation of B and M units, assume a standard atmosphere with a linear decrease of N with height and thus introduce a correction which increases linearly with height. Further studies on radio-climatology over different regions have shown that the radio-refractivity distribution is more nearly an exponential function of height [11-13]. This concept has led to the definition of a new unit that adds a correction factor to account for this exponential decrease.

Thus the $A(h)$ unit is given by

$$A(h) = N(h) + N_s \left[1 - \exp\left(\frac{-h}{H}\right)\right] \tag{15}$$

and the gradient of A can be expressed as

$$\frac{dA(h)}{dh} \quad \frac{dN(h)}{dh} + \frac{N_s}{H} \exp\left(\frac{-h}{H}\right), \tag{16}$$

where N_s = Surface refractivity and

H = Effective scale height, its value should lie between 6.5 and 7.5.

(iv) $N_0(h)$ *Unit :*

From the above discussion, it is observed that in deduction of A, M and B units, the correction terms are additive in nature. Another unit, $N_0(h)$, where the correction term is actually multiplicative in nature, can be defined by arbitrarily adopting a reduced to sea level value of refractivity. So that

$$N_0 = N_s \exp\left(\frac{+h}{7.0}\right), \tag{17}$$

where h is in kilometer. This effectively removes the station deviation dependence of N_s and allows the emphasis of air mass difference. Gradient of N_0 can be defined as

$$\frac{dN_0(h)}{dh} = \frac{dN(h)}{dh} \exp\frac{h}{7.0} + \frac{N(h)}{7} \exp\frac{h}{7.0} . \tag{18}$$

5. Classification of tropospheric refractivity gradients

Tropospheric refractivity gradient, ΔN, plays an extremely important role in the propagation of high frequency radio wave. Various workers have shown that different propagation mechanisms

can be explained on the basis of characteristics of radio-refractivity gradients, arising during different meteorological conditions [9, 14, 15]. On the basis of the magnitude and sign, the refractivity gradients can be divided into following categories.

5.1 Sub-Refraction :

When the value of refractivity gradient is > – 40N/km, it is said to be *subrefracted.* Under sub-refractive condition N instead of decreasing with height increases. As a result, the radio ray will be curved upwards (opposite in the sense of the curvature of the earth). Occurrence of sub-refractive condition may reduce the radio ranges significantly. This type of situation may occur when moisture density increases with height.

5.2 Normal Refraction :

When the value of refractivity gradient lies between – 40 N/km and – 75 N/km, the radio ray curve downwards in the same direction as the curvature of the earth surface. In this situation, N decreases with height monotonically. This condition occurs in a well mixed atmosphere which may arise due to thermal convection or wind shear.

5.3 Super-refraction :

When the value of refractivity gradient lies between – 75 N/km and – 157 N/km, radio rays are curved downwards more sharply than the normal but not as much as the curvature of the earth surface. Superrefractive gradients are formed generally due to formation of radiation inversion during night hours or due to decrease in humidity profiles. Under this condition radio ranges may be extended significantly.

5.4 Ducting :

When the value of the refractivity gradient is equal to or less than –157 N/km the atmospheric condition that arises is known as *ducting.* Under this condition the curvature of the radio ray is equal to or greater than the earth's curvature and the radio rays may travel a longer distance with less attenuation. Although it provides extended range propagation, at the same time it may account for serious interference in radar and microwave communication systems.

Various meteorological conditions, which may lead to the formation of ducting, are as follows

(i) evaporation over the sea

(ii) anticyclonic subsidence

(iii) subsidence at frontal surfaces

(iv) ,nocturnal radiative cooling over land

(v) advection and

(vi) due to some localized effects *e.g.* sea breezes and thunderstorm out flows

6. A study on radioclimatology over eastern region

Research on radio-climatology, solely depends upon the availability of meteorological observations on Temperature (T), pressure (p), humidity (e) and various other related parameters.

In India a very initial step in this regard was taken during the year 1904, when IMD (India Meteorological Department) published surface observations of meteorological parameters for 171 stations in India and neighbouring countries.

As far as the upper level measurements are concerned, *prior* to 1968, Radiosonde observations for T, p and e were available only for 12 stations at two fixed hours (0830 hrs IST and 1730 hrs IST) per day. Observations were available at a number of fixed pressure levels beginning from 900mb to 50 mb and at a number of few significant levels. Accuracy in the measurement of temperature, pressure and humidity were around 1°C, 5-10 mb and 30% respectively. During the year 1968, Radiosonde stations were increased to 18. These instruments could provide more closely spaced observations. Accuracy of data, has now been improved to 0.25°C, 2 mb and 10% respectively. Presently there are about 32 Radiosonde stations, working successfully all over India.

6.1 Brief introduction to previous work :

In India, a systematic work on radio-climatology has actually been started since 1966. In this connection, the pioneering step was taken by Kulsrestha and Chatterjee during 1966-67 when they studied the distribution of surface refractivity N_s and also the refractivity at 850 mb and 700 mb levels based on five years data at 36 surface observation stations and 12 Radiosonde Stations [16-19]. In 1968, Srivastava studied the refractivity in the lowest 1 km over India [20]. During the course of these works, the height resolution was restricted to 1 km in refractivity profiles. Venkiteshwaran *et al* (1970-72) have studied the diurnal variation of surface refractivity N_s and surface refractivity reduced to sea level, N_0 [14, 15]. In 1974, the height resolution was improved by Majumder by taking refractivity at surface and at 500 m altitude [21]. In 1978, based on 16 Radiosonde stations, Sarkar estimated refractivity gradients across 250m altitude [22]. Rao [23] and Reddy [24] have studied the radio-climatological features in southern India.

Prasad [25] has deduced the RRI (Radio Refractive Index) profiles from Radiosonde data collected from 32 station twice a day (0000 GMT and 1200 GMT) for a period of 5 years. He has also studied the radio-climatology of some selected regions over India by taking simultaneous observations from kytoon, airborne microwave refractometer and Radar.

Apart from India, work on radio-climatology is in progress in other tropical countries too. Owobabi and Ajayi [25] have reported that over Africa, the super-refractive conditions are strongest during Harmattan period (November to February). Akiyama and Sasaki [26] have deduced a combined normal exponential distribution function for refractivity gradients over Japan. Kolawole [27] has deduced the statistics of radio-refractivity for tropical climates. He has also discussed the correlation between surface refractivity and the initial refractivity gradients [26]. Bye and Howell has described the radiorefractive index profiles in super-refractive portion by a combination of logarithmic and sine function [28].

6.2 Radioclimatology over eastern coastal region of India deduced from radiosonde observations :

From the knowledge of surface refractivity over a region, one can assume the average distribution of refractivity with respect to height over that region. At the same time it can be estimated

easily from the observation of temperature (T), pressure (P) and humidity (e) at surface level. Due to these advantages surface refractivity N_s is considered an extremely useful parameter to study the properties of radio environment over a region.

Meteorological observations of T, P and e collected over Calcutta (for the year 1986 and 1987) for 0530 hrs and 1730 hrs IST, have been analyzed to estimate the value of refractivity at surface and other isobaric levels such as 950 mb, 900 mb, 850 mb, 800 mb, 750 mb and 700 mb. Yearly observations on N_s reveal that its value has remained within 275N units to 450N units. This entire range of variation has been divided into seven classes with each class having a class interval of 25N units. Percentage occurrence of N_s with respect to each class has been estimated for all four seasons (pre-monsoon, monsoon, post-monsoon and winter) over the eastern coastal region of India.

The obtained results are summarized in Tables 1 and 2. It is observed that during the monsoon season, both at 0530 hrs IST and 1730 hrs IST,

(i) N_s takes a very high value and

(ii) the percentage occurrence of N_s with respect to class 375-400N units is 83.05% and 89.98% respectively.

Table 1. Percentage occurrence of radio-refractivity at 0530 hrs IST

N_s (Unit)	Pre-Monsoon	Monsoon	Post-Monsoon	Winter
275N–300N	0.00	0 00	0 00	1.16
300N–325N	5.95	0 00	0 00	27.90
325N–350N	20 23	0 00	6 59	56 97
350N–375N	36 90	0 00	36 26	13 95
375N–400N	30.95	83 05	56 04	0 00
400N–425N	4 76	16 94	1.09	0 00
425N–450N	1 19	0.00	0 00	0 00

Table 2. Percentage occurrence of radio-refractivity at 1730 hrs IST

N_s (Unit)	Pre-Monsson	Monsoon	Post-Monsoon	Winter
275N–300N	6.17	0 00	0 00	6 89
300N–325N	24 69	0.00	2.22	43 67
325N–350N	20 98	0.00	17.17	42.52
350N–375N	35.80	3.38	34.44	6.89
375N–400N	12 34	89 98	45.55	0 00
400N–425N	0.00	6.77	0 00	0.00
425N–450N	0.00	0.00	0 00	0 00

On the other hand, the corresponding values (percentage occurrence of N_s with respect to class 375-400N units both at 0530 hrs and 1730 hrs IST) for pre-monsoon and post-monsoon seasons are 30.95% (530 hrs IST), 12.34% (1730 hrs IST), 56.04% (530 hrs IST) and 45.55% (1730 hrs IST) respectively.

Further investigation reveals that the winter season exhibits the lowest value of N_S both at 530 hrs IST and 1730 hrs IST, and the percentage occurrence of N_S with respect to the class $300N - 350N$ units is 84.87% and 86.19% respectively. Figure 15 describes the monthly variation of the average value of N_S (monthly average of dry term and wet term of N_S are also estimated). It is observed that both at 0530 hrs IST and 1730 hrs IST the average value of N_S and average value deduced on wet term of N_S experience the highest value during monsoon month followed by post-monsoon, pre-monsoon and winter months whereas monthly averages estimated on dry term of N_S have not shown any marked variability throughout the year.

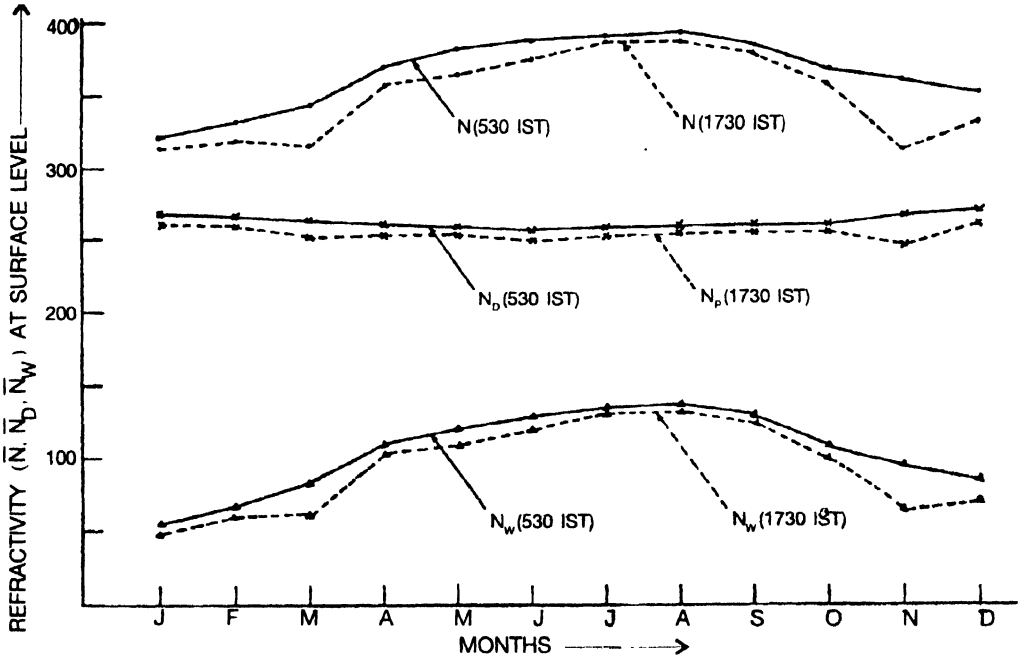

Figure 15. The monthly variation of average value of N and the average value of dry and wet term of N

6.3 Refractivity gradients :

Collected Radiosonde data are analyzed to estimate the value of refractivity gradients ΔN (with respect to surface level) at pressure levels 950 mb, 900 mb, 850 mb, 800 mb, 750 mb and 700 mb. According to the classification discussed in Section 4.6, the obtained values of refractivity gradients are classified into following categories :

1. Sub-refraction
2. Normal refraction
3. Super-refraction and
4. Ducting.

Percentage occurrence of sub-refractivity, normal refractivity, super-refractivity and ducting are estimated for all the months at 0530 hrs and 1730 hrs IST. Figures 16 to 21 describe the percentage occurrence of sub-refractivity gradients during all the months at pressure level 950 mb, 850 mb, 800 mb, 750 mb and 700 mb respectively. In these figures, solid lines are used

to join the observed values at 0530 hrs IST whereas observed values at 1730 hrs IST are connected by broken lines. It is apparent from Figure 16 that, except for the month of May, throughout the year the sub-refractive gradients are observed for a greater percent of time at

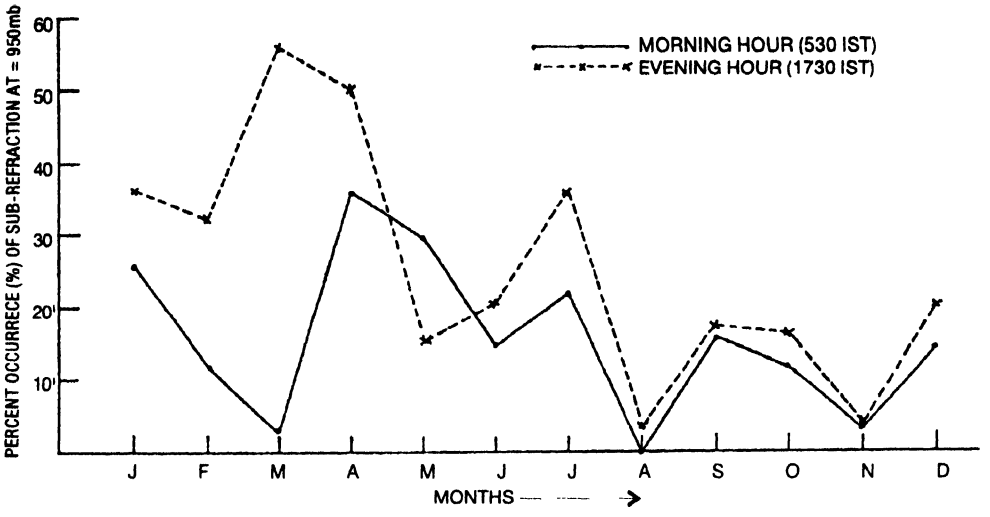

Figure 16. The monthly variation of percentage occurrence of sub-refractivity at pressure level 950 mb (with respect to earth surface)

1730 hrs IST. The month of March shows a marked difference during which at 1730 hrs and 0530 hrs IST, the percentage occurrence of sub-refractivity is 56% and 3.5% respectively. In comparison to other months both at 530 hrs and 1730 hrs IST, the percentage occurrence of sub-refractivity in negligible (lies between 0 and 8%) for the months of August and November, whereas during the month of April, both at 530 hrs and 1730 hrs IST, the percentage occurrence of sub-refractivity is 36% and 50% respectively. Figure 17 indicates that during morning hours

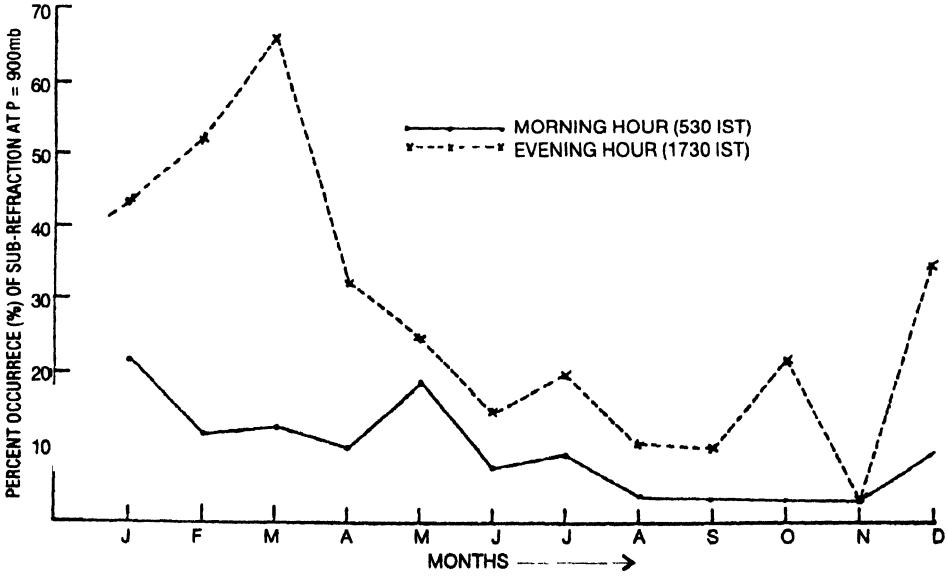

Figure 17 The monthly variation of percentage occurrence of sub-refractivity at pressure level 900 mb (with respect to earth surface).

(0530 hrs IST), at pressure level 900 mb, the percentage occurrence of sub-refractivity lies between 22% (January) and 3.5% (November) throughout the year whereas during evening hours (1730 hrs IST) it has varied between 66% (March) and 3.5% (November). Marked differences in percentage occurrence of sub-refractivity between morning and evening hours, are observed during the months of January, February, March and December. It is observed from Figure 18 that during the month of March, at 1730 hrs IST, the pressure level 850 mb

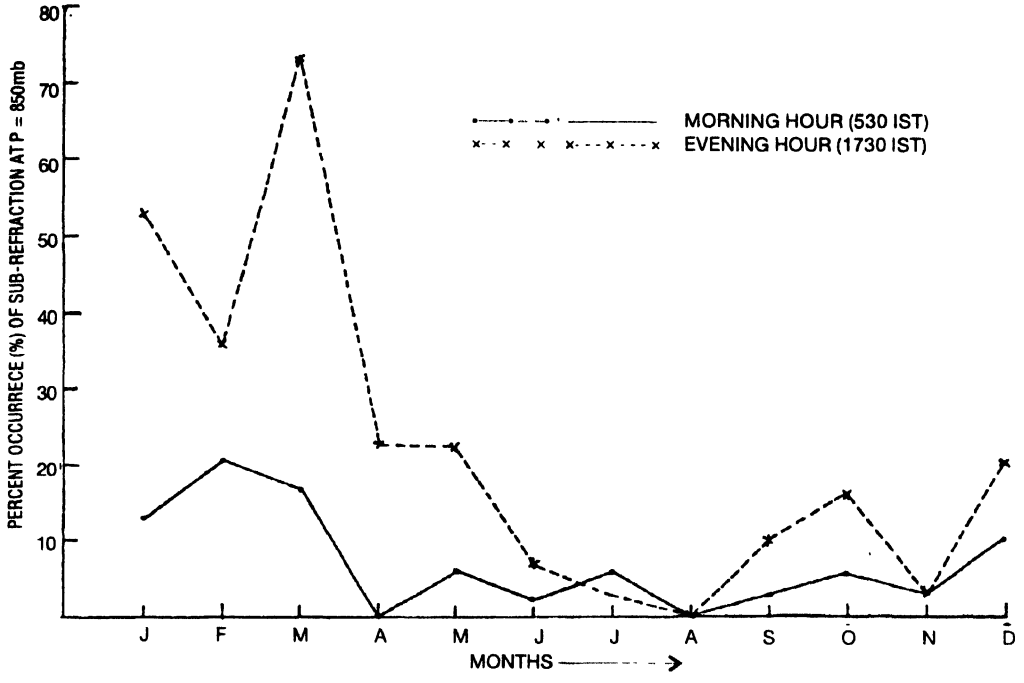

Figure 18 The monthly variation of percentage occurrence of sub-refractivity at pressure level 850 mb (with respect to earth surface).

remained sub-refractive for about 73% of the days, whereas during morning hour (530 hrs IST) the percentage occurrence of sub-refractivity varied between 0 and 21%. Further investigation reveals that both at morning and evening hours, the percentage occurrence of sub-refractivity is negligible (varied between 0 and 7.5%) during the months of June, July, August (monsoon months) and November. Figure 19 exhibits that during the month of January, February and March at 1730 hrs IST, the pressure level 800 mb remained sub-refractive (with respect to ground) for as high as 90 to 91% of the days. Similarly even at morning hour (530 hrs IST) the percentage occurrence of sub-refractivity during the months of January, February and March is 58%, 79% and 55% respectively, whereas during the months of May, June, July, August and November the percent occurrence of sub-refractivity during both morning and evening varied between 2 and 12%. Likewise, Figure 20 provides same informations as deduced from Figure 19. Once again we can observe that during the months of January, February and March (during both morning and evening) the pressure level 750 mb remained sub-refractive (with respect to ground) for a very large number of days. In contrast to this, during monsoon months during both morning and evening the percentage occurrence of sub-refractivity varied between 0 and 6%. Figure 21 reveals that during monsoon and post-monsoon seasons, both at morning and

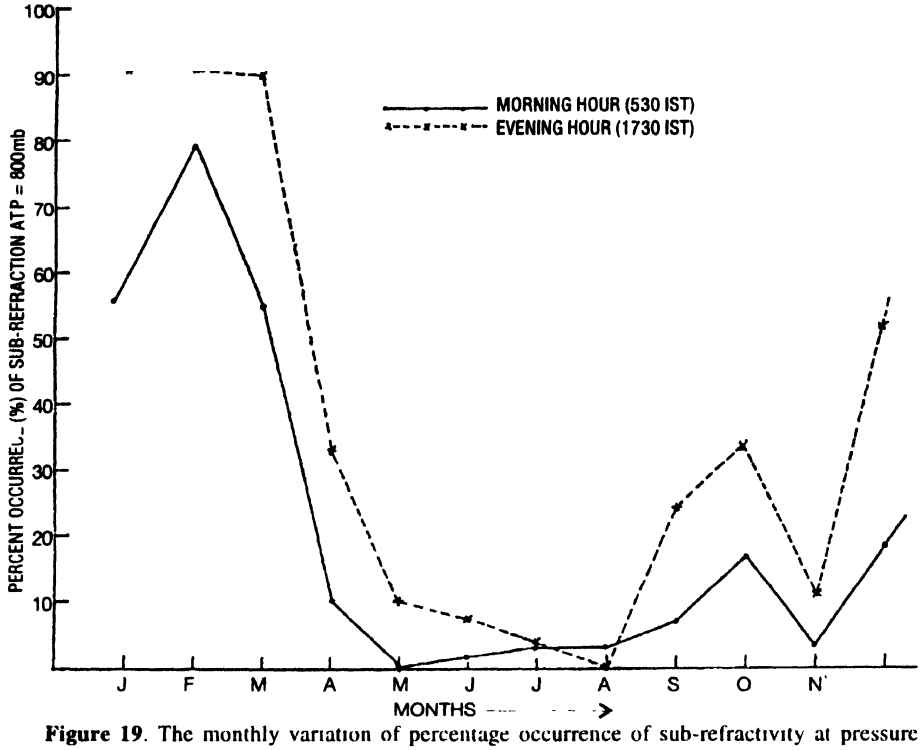

Figure 19. The monthly variation of percentage occurrence of sub-refractivity at pressure level 800 mb (with respect to earth surface)

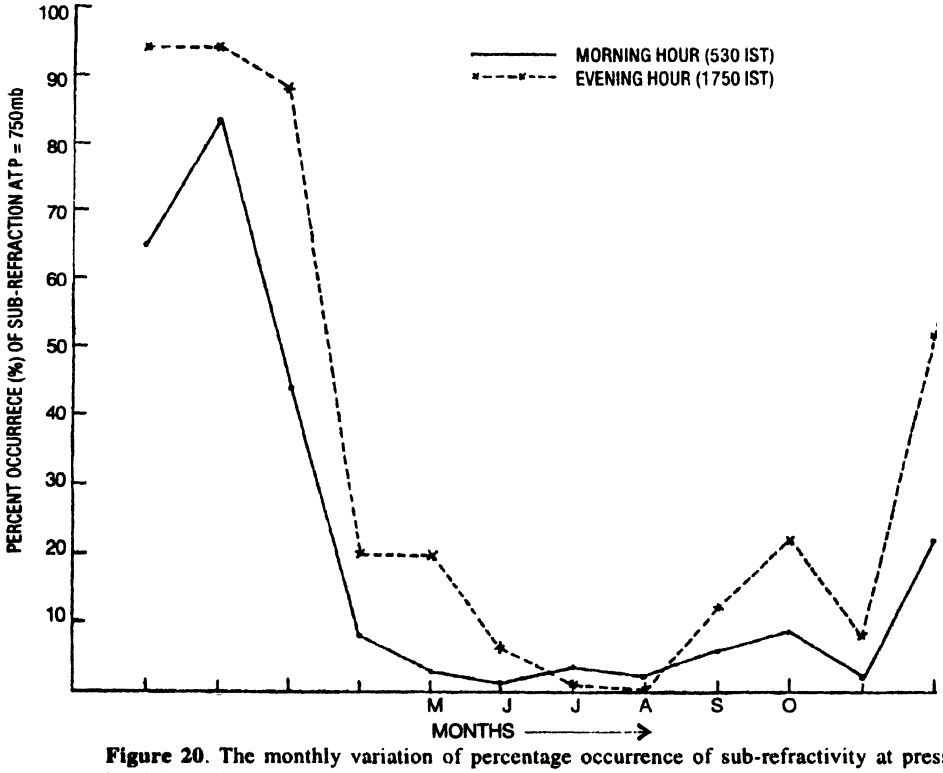

Figure 20. The monthly variation of percentage occurrence of sub-refractivity at pressure level 750 mb (with respect to earth surface).

evening hours, the pressure level 700 mb remained sub-refractive (with respect to surface) for a fewer number of days (percentage occurrence varied between 0 and 5%), whereas for winter and pre-monsoon seasons the pressure level 700 mb remained sub-refractive for about 80 to 97% of the days.

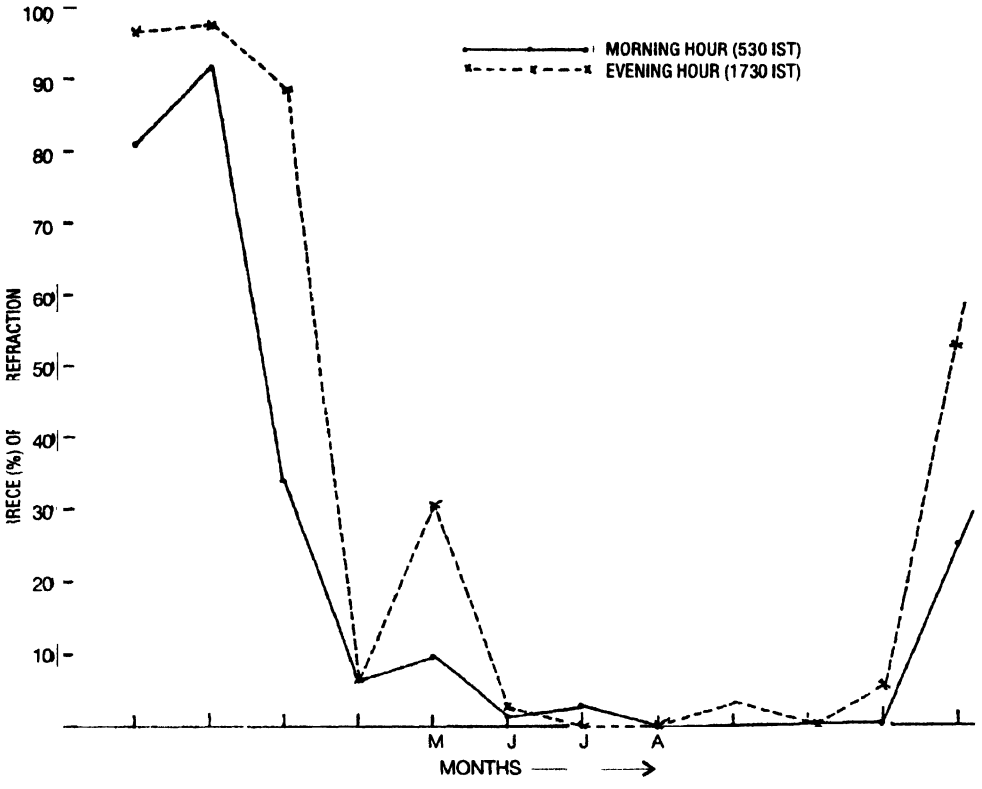

Figure 21 The monthly variation of percentage occurrence of sub-refractivity at pressure level 700 mb (with respect to earth surface).

Figures 22 to 27 describe the percentage occurrence of normal refractivity (with respect to surface) during all the months at pressure levels 950 mb, 900 mb, 850 mb, 800 mb, 750 mb and 700 mb respectively. An overall investigation on these figures reveals that the distribution of percentage occurrence of normal refractivity with respect to different months, has followed nearly the similar trends both at 530 hrs and 1730 hrs IST. Figure 22 describes that at pressure level 950 mb, the distribution of percentage occurrence of normal refractivity undergoes an oscillating behavior, with trough and crest corresponding to the months of April and August respectively. During the monsoon season, the pressure level 950 mb remained normally refractive for 55 to 75% of the days (for the both morning and evening hours), whereas the percentage occurrence of normal refractivity during pre-monsoon season remained between 13 and 35% (for the both morning and evening hours). It is apparent from the Figure 23 that during the pre-monsoon season (March, April and May) for the both morning and evening hours, the pressure level 900 mb remained normally refractive for about 26 to 46% of the days, whereas for monsoon, post-monsoon and winter seasons the corresponding ranges are 63 to 88%, 73 to 88% and 42 to 87% respectively. Figure 24 exhibits that both at 530 hrs and 1730 hrs IST the percentage

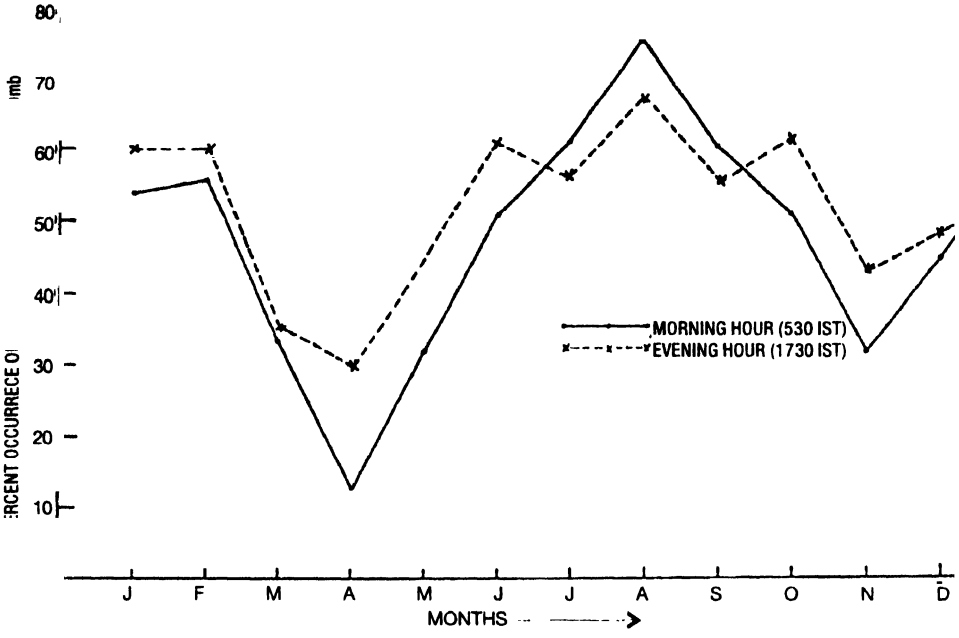

Figure 22 The monthly variation of percentage occurrence of normal refractivity pressure level 950 mb (with respect to earth surface)

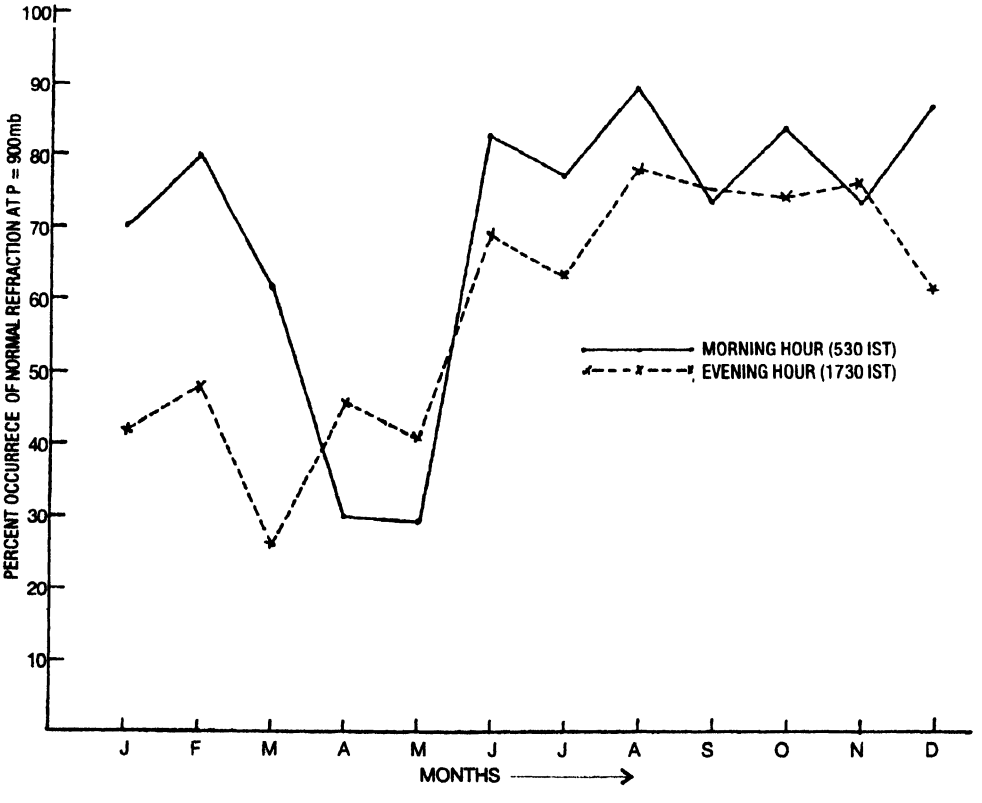

Figure 23. The monthly variation of percentage occurrence of normal refractivity at pressure level 900 mb (with respect to earth surface).

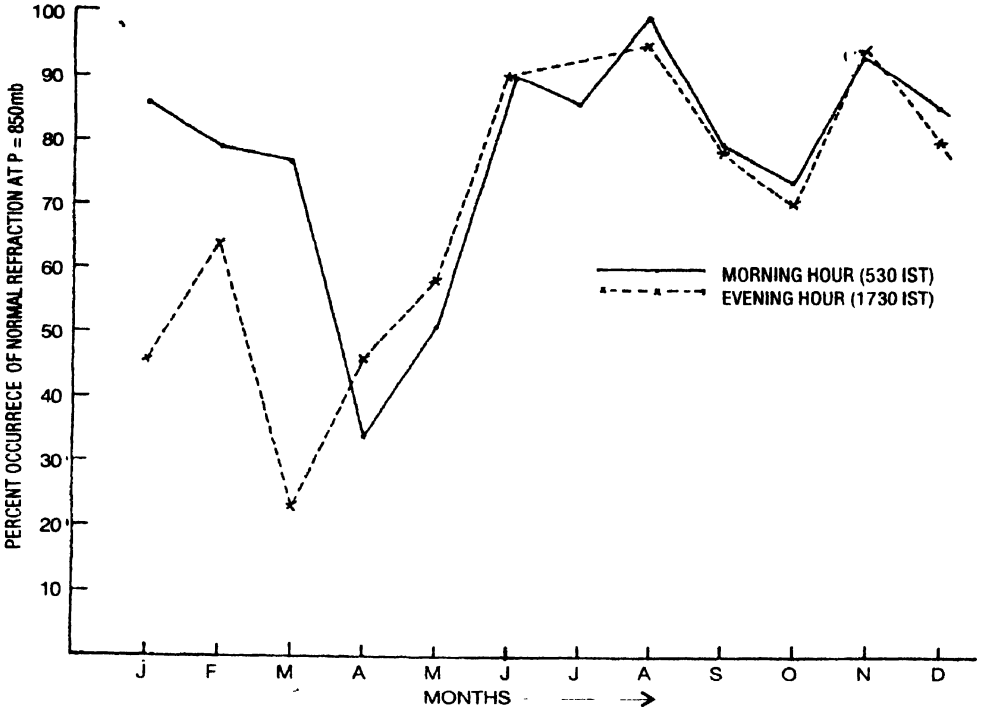

Figure 24 The monthly variation of percentage occurrence of normal refractivity at pressure level 850 mb (with respect to earth surface).

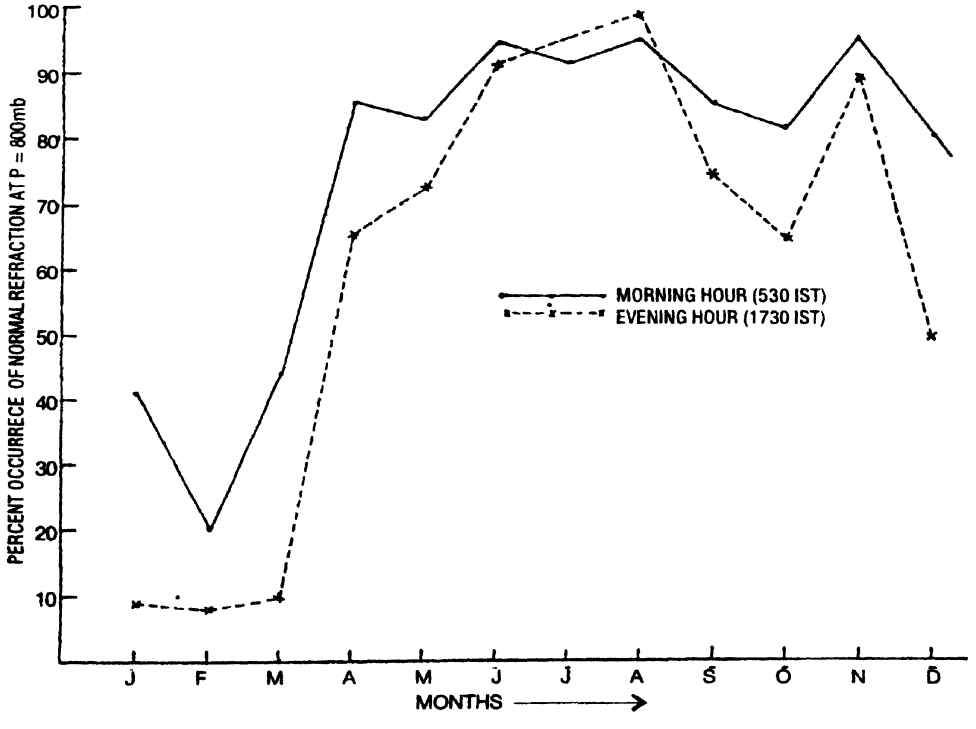

Figure 25. The monthly variation of percentage occurrence of normal refractivity at pressure level 800 mb (with respect to earth surface).

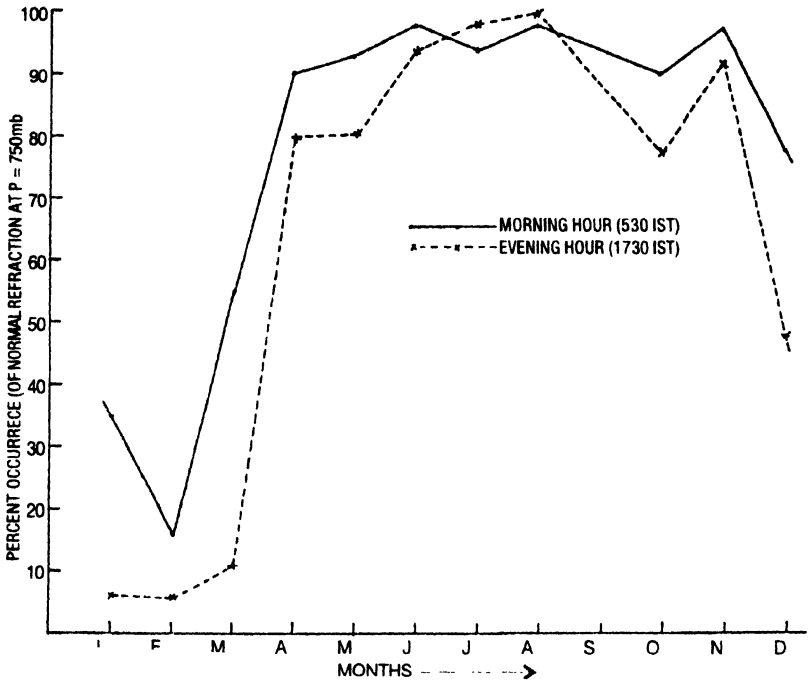

Figure 26 The monthly variation of percentage occurrence of normal refractivity at pressure level 750 mb (with respect to earth surface)

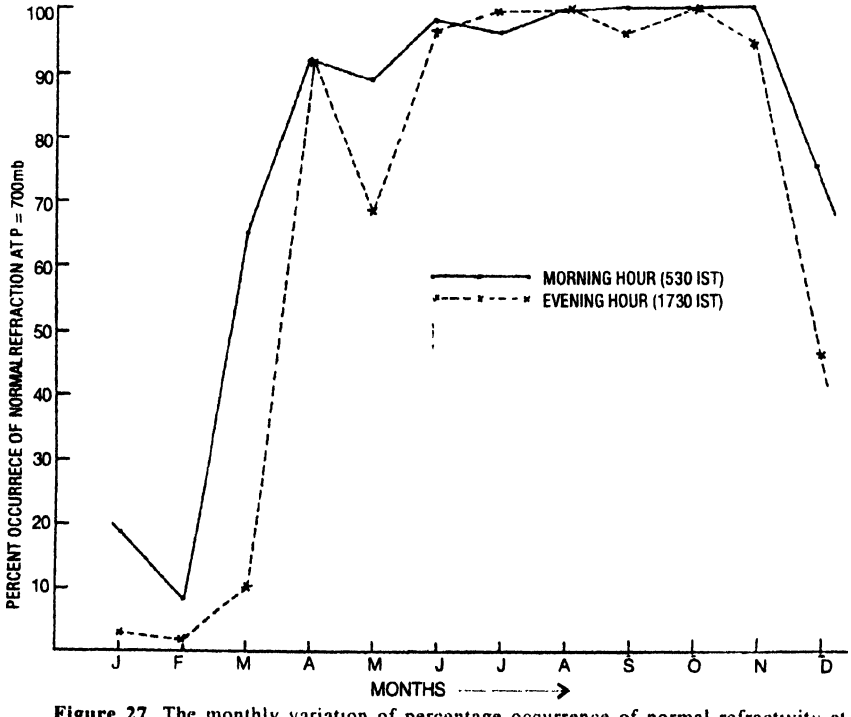

Figure 27. The monthly variation of percentage occurrence of normal refractivity at pressure level 700 mb (with respect to earth surface)

occurrence of normal refractivity is the highest during the monsoon season followed with post-monsoon, winter and pre-monsoon seasons. Finally, an investigation on Figures (25-27) reveals that except the months of January and February at 0530 hrs IST, and the months of January, February and March at 1730 hrs IST, the pressure levels 800 mb, 750 mb and 700 mb remained normally refractive for a very large number of days (during both morning and evening).

Figures (28-30) describe the monthly variation of percentage occurrence of super-refractivity (with respect to surface level) at pressure levels 950 mb, 900 mb and 850 mb respectively. It is apparent from Figure 28 that the curve for monthly distribution of percentage occurrence of super-refractivity is bimodal in nature during both morning and evening. An

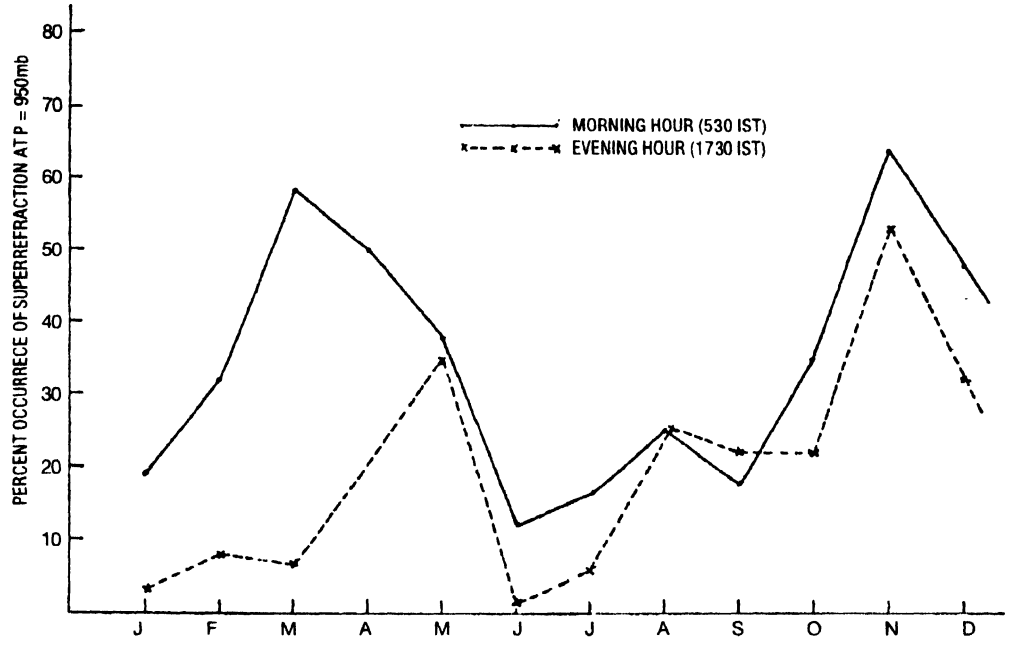

Figure 28 The monthly variation of percentage occurrence of super-refractivity at pressure level 950 mb (with respect to earth surface).

initial investigation reveals that during the morning hour (0530 hrs IST), there was a sharp increase in percentage occurrence of super-refractivity from January to March followed by continuous decrease from March to June. During the month of March for about 58% of the days, the pressure level 950 mb remained super-refractive with respect to the earth surface whereas during the month of June the corresponding percentage occurrence of super-refractivity was only 12%. From June to September, the percentage occurrence of superreactivity was fluctuated between 12 and 28%. Again a sharp increase followed with a sharp fall was noticed in the value of percentage occurrence of super-refractivity from September to November and from November to December respectively. During the month of November for about 64% of the days, the pressure level 950 mb remained super-refractive with respect to surface level. Similarly during evening hours (1730 hrs IST), the first and the second maxima were attained in the months of November (54%) and May (35%) respectively. From the January to March, the percentage occurrence of super-refractivity was varied between 3 and 7% whereas from June to October the corresponding range of variation is 2 to 30%. Figure 29 exhibits that during

morning hour (530 hrs IST) the percent occurrence of super-refractivity experienced a continuous increase from February to April, followed by a sharp decrease from the month of April to June. During the month of April about 60% of the days, the pressure level 900 mb remained super-refractive with respect to surface level whereas during the month of June the corresponding

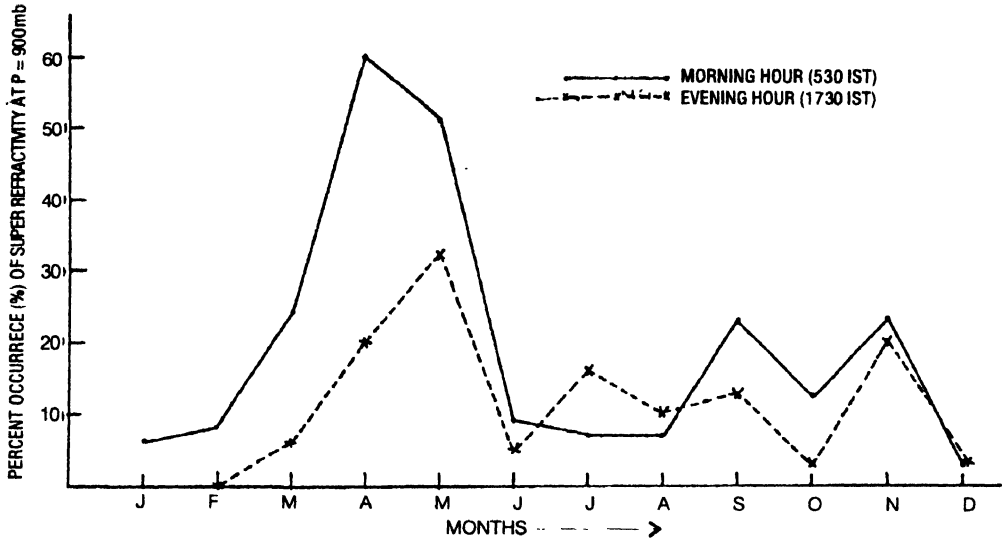

Figure 29 The monthly variation of percentage occurrence of super-refractivity at pressure level 900 mb (with respect to earth surface)

percentage occurrence of super-refractivity is only 9%. Further investigation reveals that from the month of June to December, the percentage occurrence of super-refractivity persisted between 9 and 23%. Similarly for evening hour (1730 hrs IST), the peak value of percentage occurrence of super-refractivity was observed during the month of May. During this month about 32% of days the pressure level 900 mb remained super-refractive with respect to surface level, whereas for the rest of the months the percentage occurrence of super-refractivity varied between 0 and 20%. Figure 30 describes that at 850 mb pressure level, curves for monthly distribution of percentage occurrence of super-refractivity are bimodal in nature. During morning hour (530 hrs IST), the first and the second maxima occurred in April (65%) and October (12%) respectively. Similarly for the evening hour (1730 hrs IST), the first and the second peak values were observed during the months of April (30%) and October (12%) respectively. Overall investigation reveals that at 850 mb pressure level the percentage occurrence of super-refractivity is the highest for the pre-monsoon season followed by post-monsoon, monsoon, and winter seasons (both at 530 hrs and 1730 hrs IST). Estimation of refractivity gradients (with respect to surface level) at lower pressure level *i.e.* 800 mb, 750 mb and 700 mb reveal that these pressure levels hardly become super-refractive or ducting with respect to surface level. It is evident from the earlier discussion that throughout the year these pressure levels generally remained either sub-refractive or normally refractive with respect to surface level. Tables (3-8) are presented to describe the seasonal behavior of percentage occurrence of different refractivity gradients. In these tables, M stands for the morning hour (530 hrs IST) observation whereas E describes the evening hour observation (1730 hrs IST). It is apparent from these tables that at the higher pressure levels (950 mb, 900 mb and 850 mb) the pre-monsoon and the post-monsoon seasons have remained super-refractive for a greater percent of the days in comparison with the monsoon and winter season. On the other hand, at the lower pressure levels (800 mb, 750

mb and 700 mb) all the four seasons have either remained sub-refractive or super-refractive for the majority of the days. During pre-monsoon, monsoon and post-monsoon seasons the percentage occurrences of normal refraction are greater than that of sub-refractivity gradients whereas, during winter season, percentage occurrence of sub-refractive gradient is greater than that of the normal refractivity gradient.

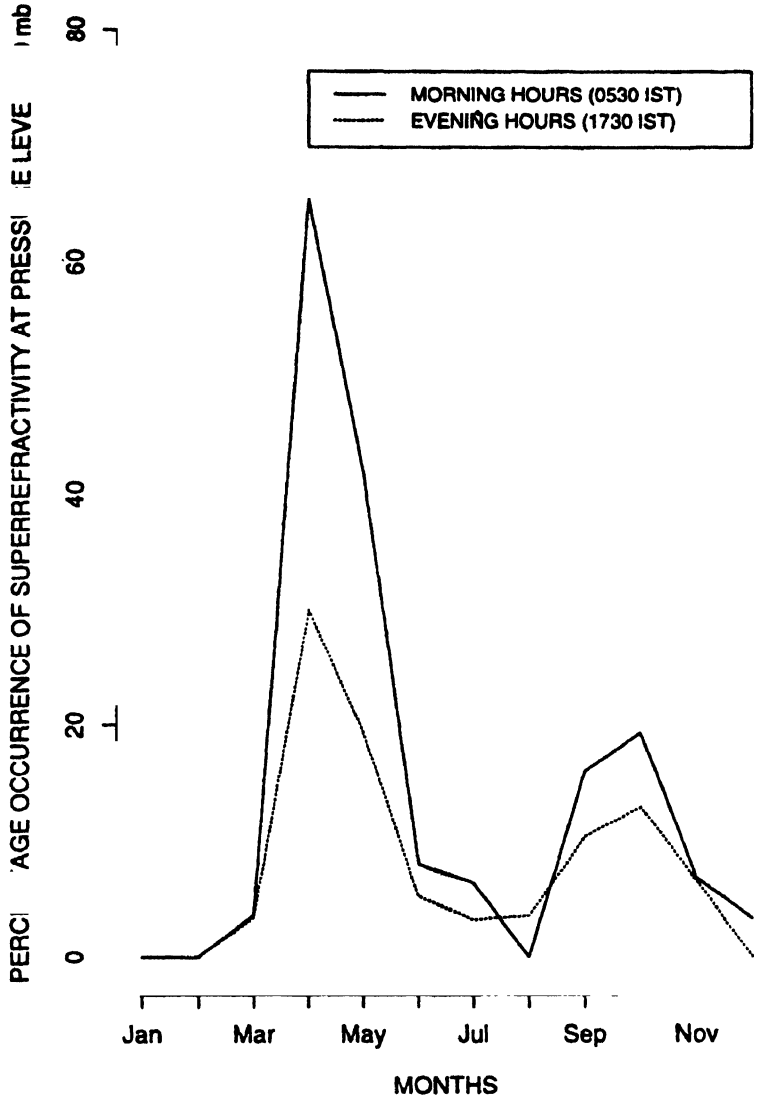

Figure 30. The monthly variation of percentage occurrence of super-refractivity at pressure level 850 mb (with respect to earth surface).

So far we have discussed mainly about the percentage occurrence of sub-refraction, normal refraction and super-refraction. From the above analysis and investigation, it is observed that at pressure level 950 mb, ducting gradients (with respect to surface level) are formed for about 3.4% of the days during the morning hours (530 hrs IST) of the month of March and for about 3.2% of days during the evening hour (1730 hrs IST) of the month of May.

Table 3. Percentage occurrence of different refractivity gradients during different seasons (at pressure level 950 mb)

Refractivity	pre-monsoon		monsoon		post-monsoon		winter	
gradients	M	E	M	E	M	E	M	E
Subrefractivity	23 04	40 92	11 29	20.12	10 59	12.23	17 39	29.33
Normalrefractivity	26 68	37 27	68.14	70 80	47.95	53 26	51 99	60.43
Superrefractivity	49 10	20 71	20 56	15 83	41 10	34 49	33 23	4.85
Ducting	1 18	1.07	0 00	0.00	0 00	0 00	0 00	0 00

Table 4. Percentage occurrence of different refractivity gradients during different seasons (at pressure level 900 mb)

Refractivity	pre monsoon		monsoon		post-monsoon		winter	
gradients	M	E	M	E	M	E	M	E
Subrefractivity	11 38	41 93	6 63	15 35	3 29	12 08	14 75	43 44
Normalrefractivity	40.36	38 08	83 35	70 95	76 84	75 57	79.35	55 47
Superrefractivity	45 24	19 63	10 02	13 68	19 85	12 34	5 89	1 07
Ducting	0 00	0 00	0 00	0 00	0 00	0 00	0 00	0 00

Table 5. Percentage occurrence of different refractivity gradients during different seasons (at pressure level 850 mb)

Refractivity	pre-monsoon		monsoon		post-monsoon		winter	
gradients	M	E	M	E	M	E	M	E
Subrefractivity	8 10	39 74	3 22	1 61	4 41	10 05	14.72	36 52
Normalrefractivity	54.88	42 67	93 54	94 98	81 28	80.09	84 16	63 47
Superrefractivity	40 33	17 56	3 15	1 70	14 08	9 96	1 11	0 00
Ducting	0.00	0 00	0 00	0 00	0 00	0 00	0.00	0 00

Table 6. Percentage occurrence of different refractivity gradients during different seasons (at pressure level 800 mb)

Refractivity	pre-monsoon		monsoon		post-monsoon		winter	
gradients	M	E	M	E	M	E	M	E
Subrefractivity	21 96	44.44	3.57	1 78	3.39	26.75	51 89	77 65
Normalrefractivity	71.50	49 99	94 63	98 21	88.65	73.23	48 03	22 34
Superrefractivity	6.42	5.56	1.19	0.00	0.00	0.00	0.00	0.00
Ducting	0.00	0.00	0.00	0.00	0.00	0.00	0 00	0.00

Table 7. Percentage occurrence of different refractivity gradients during different seasons (at pressure level 750 mb)

Refractivity gradients	pre-monsoon		monsoon		post-monsoon		winter	
	M	E	M	E	M	E	M	E
Subrefractivity	18 70	42 73	2 77	0.6	5 77	14 20	57 00	80 13
Normalrefractivity	79 61	52 82	96.00	99.40	93.96	85.80	43.00	19 90
Superrefractivity	1.61	0 00	1.25	0 00	0 00	0.00	0 00	0.00
Ducting	1.18	1.07	0 00	0 00	0 00	0.00	0 00	0 00

Table 8. Percentage occurrence of different refractivity gradients during different seasons (at pressure level 700 mb)

Refractivity gradients	pre-monsoon		monsoon		post-monsoon		winter	
	M	E	M	E	M	E	M	E
Subrefractivity	17 45	42 69	1.66	0.00	0 00	3 10	66 00	81 61
Normalrefractivity	82.55	53 96	98 34	100 0	100 0	96.89	34 00	17 39
Superrefractivity	0 00	0 00	0 00	0 00	0 00	0.00	0 00	0 00
Ducting	0 00	0 00	0 00	0.00	0 00	0 00	0 00	0 00

This is not the case that ducting gradients are not formed prominently over this region. Generally, coastal regions are extremely prone for the formation of super-refractive and ducting gradients. Actually atmospheric properties involve both spatial and temporal changes. Due to these temporal changes super-refractive gradients developed at one instant may become more negative to produce ducting gradients at other instant. It may happen that particularly at 530 hrs and 1730 hrs IST, the ducting gradients are seem to be appeared for a negligible percent of days. Present study is dependent on Radiosonde data which is available at a rate of twice daily (one at 530 hrs IST and other at 1730 hrs IST).

To compute more accurate statistics about the formation of various refractivity gradients, the upper air measurements are required at least at the rate of a set of observation per hour.

7. Summary of the Results

A. Following results are summarized from our study and observations with sodar system :

1. The mean depth of ground-based temperature inversion layer has increased between the months of January and May and it has attained the maximum value during the month of April (237.0 meters). On the other hand, it has decreased between the months of May and September and has experienced the minimum value during the month of August (137.0 meters).

2. Diurnal variation shows that mean depth of the ground-based inversion layer has increased between 1800 and 2400 hrs IST and has decreased between 2400 and 0600 hrs IST. The mean depth is the maximum between 2300 and 2400 hrs IST whereas, it is the minimum between 0500 and 0600 hrs IST.

3. Ground-based inversion layer with flat top has occurred prominently during the months of January, June and December whereas, no such kind of structures are seen to present during the months of May and August.

4. The probability of formation of ground-based layer with small spikes is higher during the pre-monsoon and the monsoon months whereas, it is lower during winter and the post-monsoon months.

5. Ground-based layer with tall spikes has formed for greater percentage of time during the months of April, May and June whereas, it has occurred for lower percent of time during the winter months.

6. The probability of formation of dot echo structure is the maximum during monsoon season followed by post-monsoon season. During winter and pre-monsoon seasons probability of formation of such kind of structures are nearly nil.

7. The pre-monsoon and the post-monsoon seasons are more prone for the formation of elevated layers whereas, during monsoon months probability of formation of these layers is very small.

8. Diurnal variation of percentage occurrence of elevated layers describes that about 66.2% of the elevated layers have occurred between 2200 and 0400 hrs IST.

9. Plot of percentage occurrence of mean depth of elevated layer suggests that more than 65% of the elevated layers have occurred between 30 and 60 meters range.

10. The probabilities of formation of wave motion in ground-based and elevated layers are higher during the pre-monsoon (generally after the departure of pre-monsoon seasonal thunderstorm) and post-monsoon seasons. On the other hand during the monsoon season probability of formation of wave motion is nearly nil.

11. Seasonal study reveals that after sunrise, to erode the ground-based layer completely the winter and the monsoon seasons take the maximum and the minimum time respectively.

12. Monthly study shows that the average time required after sunrise to erode the ground-based inversion layer is the maximum and the minimum during the months of January and June respectively.

13. Between 1100-1200 hrs IST there exist a positive correlation between average plume height and the plume duration *i.e.* taller the plume, longer the duration.

14. Between 1200 and 1300 hrs IST a continuous decrease in coefficient of correlation has been noticed and between 1300 and 1400 hrs IST there exist a negative correlation between the average plume height and the plume duration *i.e.* taller the plume, shorter the duration.

15. Between 1400 and 1500 hrs IST again there exist positive correlation between the average plume height and the plume duration *i.e.* still higher the plume height, longer the plume duration.

B. Following results are summarized from the analysis of radiosonde observations :

1. During the monsoon season, both at 0530 hrs IST and 1730 hrs IST, the surface refractivity N_s takes a very high value and the percentage occurrence of N_s with respect to class 375-400 N units is 83.05% and 89.98% respectively. This result finally concludes that the lower tropospheric boundary layer remains highly humid throughout the day and the night hours of the monsoon season.

2. Winter season exhibits the lowest value of N_s both at 0530 hrs IST and 1730 hrs IST and the percentage occurrence of N_s with respect to the class 300-350 N units is 84.87% and 86.19% respectively.

3. At pressure level 950 mb (during the morning hour) the percentage occurrence of sub-refractivity is the highest during the month of April and the minimum during the month of August whereas, during the evening hours, the percentage occurrence of sub-refractivity is the maximum and the minimum during the months of March and August respectively.

4. At pressure level 900 mb (during the morning hour) the percentage occurrence of sub-refractivity is the maximum during the month of March and the minimum during the months of August, September, October and November whereas, during the evening hours, the percentage occurrence of sub-refractivity is maximum and minimum during the months of March and November respectively.

5. At pressure level 850 mb (during the morning hour) the percentage occurrence of sub-refractivity is the highest during the month of February and minimum during the month of April whereas, during the evening hours, the percentage occurrence of sub-refractivity is the maximum and the minimum during the months of March and August respectively.

6. At pressure level 800 mb, 750 mb and 700 mb both during the morning and the evening hours, the percentage occurrence of sub-refractivity is extremely high during the months of January, February and March whereas, it is noticeably low during the months of June, July, August and September.

7. At pressure level 950 mb, 900 mb and 850 mb the percentage occurrence of normal refractivity is high during the monsoon months (June, July and August) whereas, it is low during the pre-monsoon months.

8. At pressure level 800 mb, 750 mb and 700 mb the percentage occurrence of normal refractivity is extremely low during the winter months whereas, it is noticeably high during the monsoon and the post-monsoon months.

9. At pressure level 950 mb (during the morning hours) the percent occurrence of super-refractivity is the maximum during the month of November and minimum during the month of June whereas, during the evening hours the maximum and the minimum percentage occurrence of super-refractivity has occurred during the months of November and June respectively.

10. At pressure level 900 mb (during the morning hours) the percent occurrence of super-refractivity is the maximum during the month of April and the minimum during the month of July and August whereas, during the evening hours the

maximum and the minimum percentage occurrence of super-refractivity has occurred during the months of May and October respectively.

11. At pressure level 850 mb (during both morning and the evening hours) the percentage occurrence of super-refractivity is the maximum during the month of April and it is the minimum during the monsoon months.

8. Conclusion and application

A combined study on LPBL using sodar and radiosonde techniques depicts that the percentage occurrence of ground-based and elevated temperature inversion layers (observed using sodar system) which are highly superrefractive in character (refractivity gradients estimated by analyzing radiosonde data) is high during the premonsoon and the postmonsoon season over the eastern coastal region of India. In winter season, formation of such layer take place gradually during the evening hours. A very thick ground-base temperature inversion layer forms during the late night hours and persist till next day late morning hours. From these results it can be concluded that occurrence of such layers in LPBL may provide extended range propagation (radiowave will curved downwards in the same direction as the curvature of the earth more sharply than the normal) for the radiowave lying in the high frequency band. At the same time they may cause serious interference problems in tracking the radar signals and in operating the other microwave radio-communication systems which are working over this region. During the monsoon season, a very thin temperature inversion layer is formed and the refractivity gradients lies in the normal range for a very high percentage of time. This result conclude that in this season tropospheric high frequency radiowave propagation can be achieved by having moderate path loss and at the same time probability of interference from other radio-communication systems will also be less in this season.

References

[1] J Das, A K De, N C Deb, D D Majumder, A K Sen, S K Sarkar, H N Datta and B M Reddy *Indian J Radio Space Phys* **18** 10 (1989)

[2] J Das, A K De, D D Majumder, A K Sen and S K B Mallick *Indian J Phys* **63B** 149 (1989)

[3] J Das, A K De and D D Majumder *Int. J. Remote Sensing* **10** W7 (1989)

[4] S Choudhury, D D Majumder and A Pal *Indian J Phys* **72B** 571 (1998)

[5] S Choudhury *PhD Thesis* (submitted to Calcutta University, India) 2nd April (1998)

[6] P Debye *Polar molecules* (New York Dover) (1957)

[7] J Saxton *The Anomalous Dispersion of Water Vapour at Very High Frequencies* (London . The Physical Society) Part 1-4, p 278 (1947)

[8] E Smith and S Weintraub *Proc IRE* **41** 1035 (1953)

[9] B Bean and E Dutton *Radio Meteorology* (New York . Dover) (1966)

[10] R Craig, I Katz, R Montgomery and P Rubenstein in *Propagation of Short Radiowaves* (ed. D Kerr) p.198 (New York . Mcgraw Hill) (1951)

[11] J Smith and L Trolese *Proc. IRE* **35** 1198 (1947)

[12] B Bean and L Riggs *J. Res. NBS* **63D** 91 (1959)

[13] B R Bean, L Riggs and J Horn *J. Res. NBS* **63D** 249 (1959)

[14] S Venkiteswaran and S Narayanan *Radio refractive index over India and neighbourhood for microwave propagation* (RTRC Monograph 1, National Physical Laboratory, New Delhi, India) (1970)

[15] S Venkiteswaran and V Narayanan *Diurnal variation of surface refractivity over India,* (RTRC Monograph 2, National Physical Laboratory, New Delhi : India) (1972)

[16] S Kulsrestha and K Chatterjee *Indian J. Met. Geophys.* **17** 367 (1966)

[17] S Kulsrestha and K Chatterjee *Indian J. Met. Geophys* **17** 545 (1966)

[18] S Kulsrestha and K Chatterjee *Indian J. Met Geophys* **18** 185 (1967)

[19] S Kulsrestha and K. Chatterjee *Indian J. Met Geophys* **18** 335 (1967)

[20] H Srivastava *Indian J Pure Appl. Phys.* **25** (1968)

[21] S. Majumder *Radio and Electronic Engr.* **44** 63 (1974)

[22] S Sarkar *PhD Thesis* (Delhi University, India) (1978)

[23] D Rao *PhD Thesis* (S V University, India) (1984)

[24] L Reddy *PhD Thesis* (Kakatiya University, India) (1986)

[25] M Prasad *Some Aspects of vhf and Microwave Propagation Over Selected Regions of India and Their Application to Communication* (CENTROP REPORT 50, National Physical Laboratory, New Delhi, India) (1989)

[26] T Akiyama and O Sasaki *Rev Elect Comm Labs* **27** no. 9 10 (1979)

[27] L Kolawole in *Proc URSI Comm F Symp* (Louvous, Belgium) (1983)

[28] H G D Bye in *Proc ICAP* p 229 IEE (U K) (1989)